energy&fuels

pubs.acs.org/EF
Review

Perspective on Fuel Property Blending Rules for Design and Qualification of Aviation Fuels: A Review

Published as part of Energy & Fuels special issue "2024 Energy and Fuels Rising Stars".

Randall C. Boehm, Zhibin Yang, David C. Bell, Conor Faulhaber, Eric Mayhew, Uwe Bauder, Georg Eckel, and Joshua S. Heyne*

Cite This: *Energy Fuels* 2024, 38, 17128–17145

ABSTRACT: The push toward sustainable aviation fuels (SAFs) is intensifying in response to global decarbonization efforts. This review discusses the development and assessment of probabilistic fuel property prediction methods in use today and vital for the formulation of these next-generation SAFs. We discuss the rigorous quality assurance specifications necessary for aviation fuels before they can be integrated into the supply network, with a particular emphasis on the stringent requirements for non-petroleum-based fuels or synthetic aviation turbine fuels. In this review, the relative merit of predictions based on component data and predictions derived from other modeling approaches is discussed. A total of 16 scalar products between a concentration vector (mass, mole, or volume fraction) and a property vector can be used to estimate 31 properties, counting the whole distillation curve as one property. The accuracy of these blending rules, as applied to mixtures of aliphatic and aromatic hydrocarbons in the jet fuel volatility range, is documented here. The relative contribution of blending rule accuracy to the fuel property prediction uncertainty is discussed. In most (if not all) cases, the predictive uncertainty is small relative to uncertainties arising from incomplete characterization of the component concentration or property data and/or the accuracy of reported component property data. The data used to populate the property vector comes from authoritative sources, such as the National Institute of Standards and Technology (NIST), the Design Institute for Physical Properties (DIPPR), and the periodic table of elements, or internal measurements. Additionally, the freeze point can be estimated from the crucial components' concentration and property data from a simple equation-of-state model (enthalpy, entropy, and temperature) applied to each of the crucial components. A total of 75 additional "properties" with specified criteria stated in ASTM D4054 follow directly from the measurement of trace or bulk materials or can be determined exactly from blending rules that invoke the conservation of mass. A total of 20 properties listed in ASTM D4054 are not discussed in this review. A total of 16 of the 20 properties not listed here are believed to depend upon trace level impurities (such as the jet fuel thermal oxidation test or JFTOT), lacking identification or composition data, while simple blending rules are not advised for the remainder.

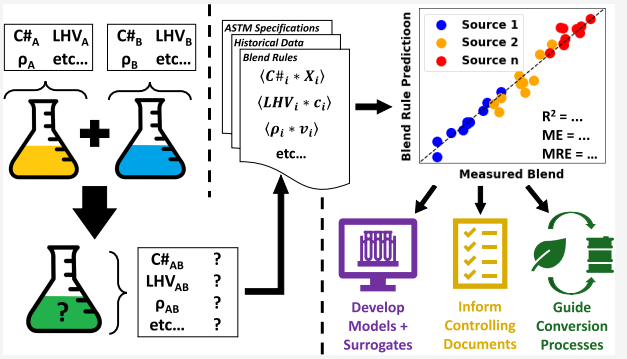

1. INTRODUCTION

The aviation industry is aggressively pursuing alternative low-carbon propulsion technologies and sustainable aviation fuel (SAF) as a means to decarbonize the sector. This shift is driven by initiatives from multiple national governments and the International Civil Aviation Organization (ICAO), which have implemented policies and challenges to accelerate the adoption of cleaner aviation solutions. As a result, there is a growing focus on developing chemical conversion technologies that can transform renewable feedstocks into jet fuel. In the United States, the SAF Grand Challenge has set an ambitious target of producing 35 billion gallons of sustainable aviation fuel annually by 2050, underscoring the urgency and scale of the decarbonization effort in the aviation industry.[1] In addition to this 2050 goal, the SAF Grand Challenge aims to facilitate the annual production of 3 billion gallons domestically by 2030, or approximately 10% of domestic jet fuel consumption.

The United States Environmental Protection Agency (U.S. EPA) reports that D4 and D6 renewable jet fuel production has seen a significant increase in recent years.[2] In 2023, 26

Received: May 23, 2024
Revised: August 17, 2024
Accepted: August 20, 2024
Published: August 27, 2024

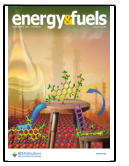

https://doi.org/10.1021/acs.energyfuels.4c02457
Energy Fuels 2024, 38, 17128–17145

million gallons of SAF were generated, and in the first half of 2024 alone, production has already reached 27 million gallons.[2] Looking ahead, domestic SAF production capacity projections are expected to surpass 2 billion gallons annually by the end of 2028.[3] This projected capacity is a substantial increase from current levels, representing nearly 80 times the production achieved in 2023. To further contextualize this growth, consider that in 2020, the combined production of biodiesel and renewable diesel, which have less stringent technical requirements compared to jet fuel, was 13.6 billion gallons.[4] The fact that SAF production is projected to reach 2 billion gallons annually by 2028, despite the more rigorous technical standards, highlights industry expectations and collective urgency of the aviation enterprise to decarbonizing.

Bridging the gap between decarbonization targets and actual production values is a substantial challenge, particularly in the case of novel SAF routes. The process of developing a new SAF pathway is both time-consuming and expensive, with an estimated cost of $100 million to produce sufficient volumes (approximately 100 gallons) of material to enter the ASTM D4054 qualification process. This qualification process alone can take multiple years, and companies may face bankruptcy along the way. Even after successful qualification and approval (resulting in an update or addition to ASTM D7566), the technology must undergo significant scale-up, initially requiring a demonstration facility before a commercial facility can be developed. These additional steps further contribute to delays and costs in the process. To align new technologies, manage expectations, and communicate likely approved blend ratios or illustrate hard limits on a given pathway's ability to produce an acceptable aviation fuel or blend stock, predictive models are employed from the inception of a novel SAF route.[5]

Currently, in the United States and Europe, aviation turbine fuels must adhere to the stringent specifications detailed in ASTM D1655 for Jet A and Jet A-1 to be considered fungible and suitable for use in the existing fuel infrastructure, aircraft, and engines. Renewable carbon can be incorporated into an ASTM D1655-compliant fuel through two primary methods: coprocessing with fossil carbon or blending an ASTM D7566-approved renewable blend component (SAF) with fossil-based fuel [it should be noted that there will likely be 100% drop-in (ASTM D1655 compliant) and non-drop-in (or Jet-X) SAF pathways in the coming years and decades]. These processes and specifications must be strictly followed to ensure that the resulting fuel containing renewable carbon meets the required standards before it can be introduced into the fungible supply network.

However, the specifications for renewable or synthetic blend components (ASTM 7566) are significantly more restrictive and rigorous compared to those for conventional fossil-based fuels. This is because fuel properties that fall outside the range defined by historical experience with Jet A or Jet A-1[6] fuel may be incompatible with existing infrastructure, including combustors, flow control logic or hardware, storage tanks, seals, handling procedures, fuel additives, and software. These heightened requirements are in place to guarantee that the introduction of renewable or synthetic components does not compromise the safety, performance, or compatibility of the aviation fuel supply.

The evaluation process (ASTM D4054) identifies and establishes appropriate property limits to control fuels made from any process/feedstock other than petroleum refining. To date, 11 conversion processes have fully passed through the evaluation process and blends of up to 10 or 50 vol % of the products of these processes with conventional jet fuel or crude oil is allowed and controlled by ASTM D7566 or annex A1 of ASTM D1655.[7] While eight processes have a corresponding annex to ASTM D7566 that ensures its production pathway is in control, there are also four "extended requirements" that apply to the finished (blended) product in addition to those called out by ASTM D1655. Further amendments to the controlling documents are expected as the blend fraction of SAF in conventional fuel increases and the diversity of commercialized SAF products potentially warrants blending multiple SAF pathways to meet the aforementioned 2030 and 2050 goals. To inform new specifications, it is important to characterize the impacts of fuel−fuel blending on the safety and performance properties of the finished product using blending rules derived from fundamental physics.

To address these challenges, it is crucial for developers of SAF to employ probabilistic fuel property prediction methods based on modest production volumes[8,9] or the anticipated composition of the considered production stream. These predictions can significantly derisk pathway development of SAF and illuminate high risk blend components early, potentially saving thousands of gallons of fuel and tens to hundreds of millions of dollars throughout the product development lifecycle, from the earliest phases to full-scale commercialization. By utilizing these prediction methods, SAF developers can ensure that their fuels meet the stringent specifications required for compatibility with existing infrastructure and engines, while also minimizing the costs and risks associated with developing new SAF pathways. Of course, for a prediction method to be useful, it is important to quantify its accuracy uncertainty. Here, information is collected from numerous, independent sources in order to document the model accuracy of simple blending rules for 17 properties, as applied to arbitrary mixtures of aromatic and saturated hydrocarbons within the jet fuel volatility range. Heretofore, no such compilation of blending rule accuracy has been published.

2. FUEL PROPERTY TARGETS

Fuel property targets based on the specifications (direct or inferred) in the controlling documents help fuel developers select target composition, feedstock, conversion approach, parameters such as pressure, temperature or catalysts used in various stages of the conversion process, biocrude refinement strategy, and blending strategy with other bioproducts or petroleum products. The financial impacts of these decisions emphasize the importance of modeling final fuel properties based on compositional data. The availability of component composition and property values of theoretical fuels can vary widely and generalized strategies for estimating model parameters that account for second order mixing effects are unknown to the authors. It is therefore difficult for researchers or developers to assemble the information required to leverage models that require input beyond composition and component property values, further motivating the use of the simplest model that affords acceptable prediction accuracy. Conversely, gaps in compositional or component property data, as required to leverage simple blending rules, can be filled by methods such as Monte Carlo sampling[5,10−12] or machine learning,[13] which facilitate a probabilistic interpretation of fuel property predictions.

https://doi.org/10.1021/acs.energyfuels.4c02457
Energy Fuels 2024, 38, 17128−17145

Table 1. Fuel Characteristic Listings

(A) properties derived from blending rules	(B) properties derived from column A	(C) composition limit specified in ASTM D4054	(D) properties impacted by trace levels of impurities or additives	(E) controlled bulk properties not covered here
carbon number, $C\#$	molecular weight, Mw	C8−C16 population distribution of aromatics (report)	conductivity versus concentration of additive	autoignition temperature
hydrogen number, $H\#$	hydrogen to carbon ratio, H/C	C8−C16 population distribution of paraffins (report)	corrosion of copper	hot surface ignition temperature
density, ρ	percent hydrogen, $\%H$	copper	distillation loss	upper flammability limit
lower heating value, LHV	molar volume, V_m	cycloalkanes	distillation residue	bulk modulus versus temperature and pressure
heat capacity, C_p	higher heating value, HHV	existent gum	effect on clay filtration	
thermal conductivity, k	energy density, ED	fatty acid methyl esters	effect on coalescer filters and monitors	
kinematic viscosity, ν	isentropic expansion factor, γ	halogens	electrical conductivity	
surface tension, σ	thermal diffusivity, α_H	mercaptan sulfur	lubricity	
freeze point, T_{fp}	dynamic viscosity, η	naphthalenes	microseparometer rating	
vapor pressure, P_{vap}	Prandtl number, Pr	nitrogen (fuel bound)	potential gums	
distillation curve (ASTM D2887, infinite-plate limit), Tn	Ohnesorge number (fuel-dependent terms), Oh'	peroxides	response to CI/LI additive	
lower flammability limit, LFL	distillation curve (ASTM D86, one-plate limit), Tn	polar organic molecules (report 13 classes)	thermal stability	
flash point, T_{flash}	refractive index, n	tetralins and indanes	water solubility versus temperature	
dielectric constant, ε	smoke point, S_p	total acidity	compatibility with additives	
threshold sooting index, TSI		total aromatics	toxicity	
derived cetane number, DCN		total sulfur	air solubility	
elastomer swell, Sw		trace elements (22 listed at <100 ppb)		
		water		
		antioxidant (approved additive)		
		metal deactivator (approved additive)		
		fuel system icing inhibitor (approved additive)		
		electrical conductivity improver (approved additive)		
		leak detection tracer (approved additive)		
		biocide (approved additive)		
		corrosion inhibitor/lubricity improver (approved additive)		
		water scavenger (approved additive)		

Multidimensional optimizations employed for distillation cuts,[14] conversion process parameters,[15] specification alteration trade studies,[16] etc. may invoke blending rules millions of times, magnifying the impact of computational time. In this context the functional requirements on the chosen blending rules may be skewed more toward ease of use and less toward accuracy than the functional requirements on the chosen blending rules applied to a less generalized outcome. For example, fuel surrogate development[11,17,18] is all about matching a suite of properties of very complex, natural fuels to those of engineered surrogates, comprised of few (<25) components that are readily procurable in high-grade purity. Throughout their development cycle, surrogate fuels (real or imagined) have no gaps in component property or composition data, and it may be possible to assemble the information necessary to incorporate second order mixing effects into the property predictions. Since surrogate defining routines iterate across a relatively small number (<25) of plausible constituents, blending rules may be invoked thousands of times instead of millions, as required for optimizations iterating across many (∼1150) plausible constituents, and thus the impact of model computational time is minor. Presumably, the more complex fundamental models improve the probability of attaining a match to all of the chosen property targets on the first attempt. In contrast, simple blending rules facilitate complex optimizations and expedite the flow of important information between aviation fuel stakeholders.

Within the context of modeling, composition-property relationships can be distinguished by three distinct categories. The first category treats the fuel as a singular entity, predominantly employing machine learning or regression techniques.[13,19−23] These models stand out for their exemption from requiring blending rules, although their applicability is confined to fuels similar to those in their training data sets. The second category, in contrast, perceives fuel as a mixture of various components. It necessitates not only precise blending rules but also comprehensive data on all constituents present in the fuel. The third category represents a hybrid approach.[13,22,24−26] It conceptualizes fuel as a "mean component". This category is distinguished by its training on both fuels and individual components, enabling it to autonomously learn the blending rules required for accurate analysis. The second category has an advantage in terms of accountability and also on extrapolation to unknown fuels. In this paper, we examine the blending rules, since they are, besides accurate

https://doi.org/10.1021/acs.energyfuels.4c02457
Energy Fuels 2024, 38, 17128−17145

data of all constituents of the fuel, crucial for models of the second category.

Within the first category, fuel properties can be estimated from regression models that relate a set of measured properties, e.g., nuclear magnetic resonance (NMR), Fourier transform infrared (FTIR), Raman, etc., to the properties of interest. An excellent review of these methods has been reported by Vozka and Kilas in 2020[27] and the points made there will not be repeated here, except as needed. These models suffer from, not only an undetermined isomeric population distribution but also an undetermined distribution of carbon number within each family. Moreover, certain properties, the distillation curve for example, are strongly impacted by characteristics that are not significantly informed by the optical or magnetic properties of the mixture, and thus cannot be predicted by any model that exclusively uses such data to inform the model. The other fundamental issue with regression models is that input to the model would be very difficult to determine without making a physical measurement, and thus composition optimizations, involving property estimates for millions of composition variants, would be extremely difficult or problematic to execute.

Regarding simple blending rules of the second category, 16 scalar products between a concentration vector (mass, mole, or volume fraction) and a property vector can be used to estimate 31 properties, including a nominal predicted value and confidence intervals. The goal of this review is to document the uncertainty of these models when applied to mixtures of hydrocarbons that are potentially significant components in jet fuel; C7−C18 alkanes and aromatics. These scalar product models apply to mixtures of complex fuels as well as mixtures of pure components and everything in-between, which is particularly valuable for anticipating fuel properties in advance of blending fuels from different sources. Additionally, one model that is somewhat more complex than a scalar product will be discussed. Each of the property models to be discussed in this review is listed in column A of Table 1 while column B provides a listing of other relevant properties that can be determined from those listed in column A. Most of these property-property relationships are exact; the uncommon exceptions are discussed in section 3.

In addition to physiochemical properties, ASTM D4054 also addresses the concentration of certain elements, molecules or types of molecules, and these are listed in column C of Table 1. Of course, measurements are required to acquire this data for real fuel samples, but for conceptual fuels or blends of component fuels that have fully characterized composition, the obvious blending rules are exact.

Column D of Table 1 lists fuel properties that are controlled by ASTM D4054 and influenced significantly by certain types of impurities that may be present in some aviation fuel samples at less than 1%m. While it may not be possible to estimate these properties from detailed composition, it may be possible, in some cases, to predict the outcome of blending two or more fuels for which the property of interest was measured. No attempt is made here to document or assess any such model.

Column E of Table 1 lists four properties which are theoretically predictable from detailed bulk composition characterization, but which are not predicted well by simple blending rules. The models required to make predictions of autoignition temperature or a hot surface ignition temperature should involve detailed chemical kinetics and fully described temperature, pressure and gas phase species concentrations as a function of time. The upper flammability limit (UFL) can be estimated by using a model similar to that used for the lower flammability limit, but some of the approximations used in that model do not hold at relatively high fuel concentration. Intuition suggests that better estimates of UFL could be attained from more comprehensive, yet unparameterized physical models. The bulk modulus of fuels at standard temperature and pressure could be predicted well by a simple blending rule that employs component concentration and property data inputs; however, such a model is not expected to hold at conditions (temperature and pressure) approaching a phase boundary or at supercritical conditions. While the prediction of each of these four properties is certainly interesting and important, a characterization of the generality and accuracy of available (or developing) models is beyond the scope of this review.

While columns C−E of Table 1 contribute to its convenient compilation of important jet fuel properties, the focus of this review is on documenting the accuracy of and generality of the blending rules that can be used to predict the fuel properties listed in column A and the property-to-property relationships (or definitions) that can be used to predict the fuel properties listed in column B. In most applications the uncertainties of these blending models are small compared with the uncertainties introduced by the values of their inputs. For example, Hall et al.[28] have recently published an excellent presentation of properties of C8−C16 hydrocarbons from which the undetermined isomer uncertainty term can be inferred, and an approach (also known as category 3) taken to reduce this uncertainty has been described elsewhere.[8,9] The uncertainty introduced through incomplete property vectors boils down to the accuracy of a quantitative structure−property relationship (QSPR) model or the accuracy of the model used to describe the temperature dependence of the property. Citations to important works describing these models will be provided in the discussion section. Promising recent advances in the approach for developing QSPR models have been proposed by Pan et al.[29] and a thorough discussion of prior work on this topic has been provided by Landera et al.[30] Here the focus is on blending rule uncertainty, so discussion of models used to get component property data is limited.

A partial assessment (2 data points) of models available for the prediction of four important fuel properties has recently been given elsewhere.[31] Here, the focus is on documenting model uncertainty for every property of interest to the stakeholder community, and to juxtapose that uncertainty term with other sources of uncertainty in predictions. As such, each of the blending rules foreshadowed by Table 1 is documented in the discussion section, along with a characterization of its accuracy. Uncertainties are communicated with a unity plot when available, and by a standard deviation (σ), a mean absolute error, or a mean error. Unless there is reason to believe otherwise, quadrature addition of random error originating with each term in the scalar product is assumed for multicomponent mixtures, and in the absence of any evidence to the contrary we assume the variance of each term depends linearly on its concentration alone as described by eq 1. Evidence supporting the validity of this assumption is included or cited in the discussion section relating to some of the blending rules.

Property/property relationships (formulas) are also documented within the same subsection as the blending rule(s) that

https://doi.org/10.1021/acs.energyfuels.4c02457
Energy Fuels 2024, 38, 17128−17145

serve as source terms them, and the accuracy of the approximate (or empirically motivated) property/property relationships are qualified but not quantified. Generally, the uncertainty terms applicable to these relationships are also estimated by quadrature addition as represented by eq 2, where property Z is a function of properties, x_1 and x_2.

$$\sigma_{\text{mix}}{}^2 = \sigma^2 \sum_i \tilde{c}_i{}^2 \mid \tilde{c}_i = \min(c_i, (1 - c_i)) \tag{1}$$

$$\sigma_Z{}^2 = \left(\frac{dZ}{dx_1}\right)^2 \sigma_{x_1}{}^2 + \left(\frac{dZ}{dx_2}\right)^2 \sigma_{x_2}{}^2 \tag{2}$$

3. BLENDING RULE SELECTION, GENERALITY, AND ACCURACY DOCUMENTATION

3.1. Conservation of Mass. The average number of carbon or hydrogen atoms per molecule in a mixture is determined exactly by the scalar products expressed as eq 3. In these identities, $\vec{X}$ is the mole fraction vector, $\vec{C}_n$ is a vector of integer values corresponding to the number of carbon atoms characterizing the concentration bin (from the stenciled region of a chromatogram) and $\vec{H}_m$ is a vector of integer values corresponding to the number of hydrogen atoms characterizing the concentration bin. While these models introduce no error whatsoever, there is some uncertainty attributed to their inputs.

$$C\# = \langle \vec{X} | \vec{C}_n \rangle \text{ and } H\# = \langle \vec{X} | \vec{H}_m \rangle \tag{3}$$

The undetermined isomer uncertainty as well as the component property value uncertainty are zero in these models, whenever the input data applies to discrete molecules or bins of molecules (isomers) having the same empirical formula. In these cases, the only uncertainty entering into predictions of carbon number ($C\#$) and hydrogen number ($H\#$) is that associated with the concentration vector, which typically comes from a GC × GC experiment. While the GC × GC analytical approach has already garnered widespread use and value, the effort to standardize it to group types quantification of hydrocarbons[32] is in its infancy. This complicates uncertainty determination, but lab to lab reproducibility tests have been performed[33] and are expressed here as eq 4, which fits their published reproducibility data. The true uncertainty could be larger due to bias consistent across experiments, such as FID response factor inconsistencies,[34] stencil errors, volatility overlap between isomers in different hydrocarbon families, column health, numerical peak integration bias, unnoticed retention time wrap-around, etc. That being said, there are also factors that could render the error smaller such as the fact that the concentration vector must sum to one and the high likelihood that miss-appropriated peaks on a chromatogram, the main source of error, would be off by a single carbon number. For chromatogram stencil bins that encompass thousands of isomers, such as C15 isoalkanes for example, it is possible to miss a large fraction of the mass in the bin if many of the isomers are present at a concentration that is below the detection limit of the experimental method.[35]

$$\sigma_y = 0.26\bar{y}^{0.28} \tag{4}$$

Armed now with $C\#$ and $H\#$, the hydrogen to carbon ratio (H/C) can be determined without any uncertainty contribution from the model itself, which is, as its name implies, a straightforward ratio, documented as eq 5. This property is used in correlation-based models for lower heating value and sooting propensity as well as physical models of combustion products. The average molecular weight of the molecules comprising a fuel sample is given by eq 6, where 1.008 g/mol is the atomic weight of hydrogen and 12.011 g/mol is the atomic weight of carbon, and the fuel's mass fraction of hydrogen is documented by eq 7. A fuel's molecular weight is used to convert between mass and mole concentration units and to convert between density and molar volume, which is discussed in the next subsection, while the mass percent hydrogen is used in the conversion of higher heating value, HHV (i.e., gross heat of combustion) into lower heating value, LHV (i.e., net heat of combustion).

$$H/C = H\#/C\# \tag{5}$$

$$\text{Mw}_{\text{fuel}} = 12.011C\# + 1.008H\# = \langle \vec{X} | \overrightarrow{\text{Mw}} \rangle \tag{6}$$

$$\%H = 1.008H\#/\text{Mw}_{\text{fuel}} \tag{7}$$

3.2. Ideal Solution. It is well-known that solutions do not always blend linearly, and the resulting density of a combination of two fluids is not the simple weighted average of the two. Nevertheless, the approximation represented by eq 8 is documented here because of its simplicity and because the uncertainty it introduces into jet fuel property predictions is small compared to uncertainty originating from the model inputs. In this equation, V_{m} is molar volume, ρ is density, and $\vec{\nu}$ is the concentration vector in terms of volume fractions. The denominator used for volume fractions is the sum of component volumes, not the mixture volume, and thus $\vec{\nu}$ is a unit vector.

$$V_{\text{m,fuel}} = \langle \vec{X} | \vec{V}_{\text{m}} \rangle \text{ or } \rho_{\text{fuel}} = \langle \vec{\nu} | \vec{\rho} \rangle \tag{8}$$

$$\sigma = 0.007\rho_{\text{fuel}} \sqrt{\left(\sum_i \tilde{\nu}_i{}^2\right)} \mid \tilde{\nu}_i = \min(\nu_i, (1 - \nu_i)) \tag{8.1}$$

A unity plot showing 146 recently published[36] measurements and predictions of density at 15 °C of two-constituent mixtures of species likely to be found in jet fuel is shown in Figure 1. In this data set each constituent may be a single component, a 50:50 by volume blend of single components or a complex mixture such as jet fuel. The largest modeling errors are observed when the final mixture contains two or three species which is consistent with the presumption expressed by eq 1. The standard deviation of the model error is given by eq 8.1 and is consistent with previous determinations made from more limited data sets.[37] In comparison, a recently published regression model imbued with composition data from GC × GC−FID experiments attained 0.1% mean absolute percentage error.[38] In contrast, the standard deviation of the distribution of molar volumes applicable to a given hydrocarbon class is approximately 10% of the mean for that class.[28] Moreover, the uncertainty in the density prediction is very small relative to the acceptable range for jet fuel which is 0.775−0.840 g/mL. Even for compositions identified with full isomeric detail, where the model error is not dwarfed by its input uncertainty, having a prediction uncertainty that is less than 1% of the nominal prediction is hardly motivation to seek out a more accurate model in the applications of note here. Nonetheless, readers who are interested in more accurate mixing rules to

https://doi.org/10.1021/acs.energyfuels.4c02457
Energy Fuels 2024, 38, 17128−17145

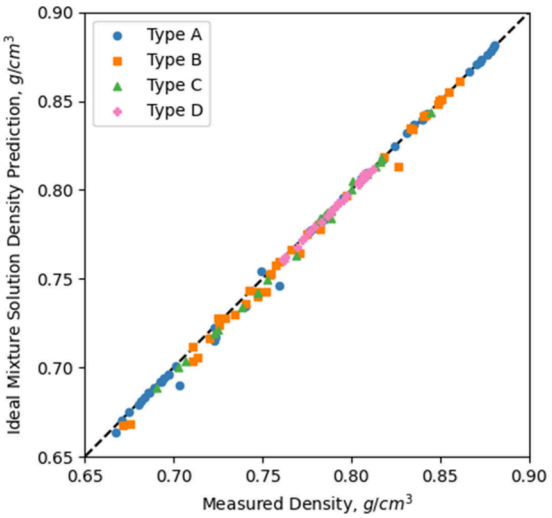

Figure 1. Unity plot for ideal solution approximation. Binary mixtures of aliphatic and aromatic hydrocarbons within the jet fuel volatility range. Type A: Both mixture constituents are comprised of a single component. Type B: One mixture constituent is a single component; the other is a 50:50 (by volume) mixture of two components. Type C: One mixture constituent is a single component; the other is a complex mixture. Type D: Both mixture constituents are complex mixtures.

predict the density (or molar volume) of fuels may consult Nabipour et al.[39] as a starting point.

The fuel density is a fundamental property to which many other properties are correlated, notably for aviation including speed of sound and dielectric constant, which are measurements taken in flight, along with fuel volume to gage fuel mass and latent heat available to power the aircraft. The density of the fuel that is in an aircraft should be known as accurately as possible, through direct measurement, primarily for this reason. Pre-application, however, equipment manufacturers design their hardware to accommodate any fuel that conforms to the specification range, 0.775−0.840 g/mL at 15 °C. From the perspective of SAF developers, that is the target, period. The density estimates noted here are used to guide blending formulations and as input to several other property estimates as discussed below, which are also driven by a target range. It is presumed here that a <1% prediction error is small compared to the margin producers develop between the fuel specification limits and the property goals they set internally for their product.

3.3. Conservation of Energy. Enthalpy (per unit mole or mass) is a state function and therefore the change in enthalpy between any two states of the system is not dependent on the path taken to connect them. This, of course, applies to heats of formation, heat of combustion, and the general form of the exact blending rule is given by eq 9. In this expression ΔH refers to a change in enthalpy, c refers to the units of the concentration vector (mass or mole) and ΔH_{mixing} refers to the heat of mixing. For the liquid phase, the heat of mixing is not quite zero in real mixtures, and by neglecting this contribution in the application of eq 5 a negligibly small error, expressed by eq 9.1, is introduced. The values reported here are based on the measurements of Lundberg.[40] Boehm et al.[41] discussed in detail the other sources of uncertainty in the so-called "tier alpha" method as applied to 17 different complex mixtures. While the modeling error received a mention in that article, it contributes ∼100 times less than the measurement uncertainties of the component concentrations and enthalpies and ∼1000 times less than the uncertainty attributed to undetermined isomers.

$$\Delta H_{c,fuel} = \langle \vec{c} | \Delta \vec{H}_c \rangle + \Delta H_{mixing,c} \tag{9}$$

$$\Delta H_{mixing,kg,liq} = 0.0 - 0.3 \text{ kJ/kg} \tag{9.1}$$

Equation 9 applies to the higher and lower heating values, HHV and LHV of the fuel (also known as gross and net heat of combustion) as well as the gas or liquid phase heat of formation, any of which may be used in engineering models applied to combustion, engine performance and aircraft drag. The product of LHV with (mass) density yields the energy density (ED, eq 10) which may be used in engineering models to determine volumetric flow rates, fuel system pressure losses, and heat transfer, for example. For specialty SAF (not conforming to ASTM D1655) the energy density of the fuel would also be used for fuel passage and orifice sizing as well as airplane fuel tank sizing.[16]

$$ED_{fuel} = LHV\rho_{fuel} \tag{10}$$

The temperature derivative of eq 5 results in the heat capacity, C_p, and this is expressed as eq 11, where the derivative of the heat of mixing term has been dropped as an approximation. The uncertainty introduced by this approach is negligible in the gas phase because intermolecular forces do not significantly perturb the saturated degrees of freedom of motion associated with molecular translation and rotation or the largely unsaturated degrees of freedom of motion associated with intramolecular vibrations. In the liquid phase however, none of these assertions are true. The degrees of freedom associated with "hindered" rotation of molecules or intermolecular (or lattice) vibrations (sourced back to translation and rotation of gases) contribute significantly to its temperature-dependent heat capacity and these lattice vibrations are wholly determined by intermolecular forces which are certainly different for heterogeneous terms (the left side of eq 11) than they are for homogeneous terms (the right side of eq 11). The impact of these intermolecular forces is referred to here, and in the cited literature, as excess heat capacity.

A total of 81 measurements of binary aromatic hydrocarbon blends have indicated that the contribution of excess heat capacity is within ±0.9% of the bulk fluid heat capacity.[42] Beyond this example, the vast majority of work related to the evaluation and prediction of multicomponent liquid heat capacity is focused on polar molecules, which are present only in trace amounts in aviation turbine fuel. Sharma et al.[43] observed a maximum 12.8% deviation from eq 11 for 803 total heat capacity measurements of binary and ternary polar compound mixtures. This is consistent with 1083 measurements by Malik et al.,[44] who reported a maximum 12.5% contribution of mixing toward the bulk fluid heat capacity, as well as earlier studies.[45,46] In both the polar and nonpolar studies cited here, blend ratios containing large mole fractions of multiple components (e.g., 0.5/0.5 binary or 0.45/0.45/0.1 ternary ratios) exhibited the highest excess heat capacity supporting the application of eq 1 to the heat capacity blending rule. Since this has not been proven and it is unclear whether trace polar molecules may have a disproportional impact on heat capacity, the evaluation of heat capacity for complex mixtures, such as aviation turbine fuels, represents an area of fuels research in need of attention. Nevertheless, the discussion

https://doi.org/10.1021/acs.energyfuels.4c02457
Energy Fuels 2024, 38, 17128−17145

in the following paragraph applies under the assumption that eq 1 is applicable to the heat capacity blending rule when applied to aviation fuels.

$$C_{p,c,fuel} = \langle \vec{c} | \vec{C}_{p,c} \rangle \tag{11}$$

$$\sigma \approx 0.06 C_{p,c,fuel} \sqrt{\left(\sum_i \tilde{c}_i^{\,2}\right)} \mid \tilde{c}_i = \min(c_i, (1 - c_i)) \tag{11.1}$$

At first blush, an error of 12.5% is concerning because accurate heat capacity is necessary (but not sufficient) to execute accurate heat transfer analyses of fuel systems to get accurate fuel temperature and enthalpy at inlet to the fuel nozzle and the combustor, where fuel temperature also impacts, exponentially, viscosity and thermal stability of fuel. However, upon closer inspection, the estimated uncertainty of eq 11 for many component mixtures is less concerning. Assuming the 12.5% max observed error of 1083 data points (215 mixtures) is three standard deviations off and the mean error is zero, then the random error in the heat capacity prediction is given by eq 11.1. The leading scalar, 6% is still concerning, but the sum of the square of the mole fractions is a small number for many component fuels. Even for SAF with very few components, which are typically limited to a maximum blend ratio of 10 vol % with a conventional jet fuel, the sum of the mole fractions squared is unlikely to exceed 0.028, below which the standard deviation of the model error is less than 1%.

Returning now to the gas phase, for which the error in eq 11 is negligible, there is little interest in knowing the heat capacity of vaporized jet fuel, as it along with the fuel latent heat of vaporization is baked into the LHV application of eq 9. A rare demand for the vaporized fuel heat capacity occurs during detailed redesign of premixing chambers within combustors, where fluid dynamics is very complex, but temperature gradient estimates which employ fuel vapor heat capacity are necessary to illuminate potential root cause of observed coking or autoignition issues that show during a design validation test.

The heat capacity of the combustion products is more interesting than the heat capacity of vaporized fuel under normal circumstances, as it is used to calculate adiabatic flame temperature. The combustor exhaust gas heat capacity, more precisely the ratio of the temperature derivatives of enthalpy and internal energy at constant pressure (C_p) and volume (C_v) respectively, should be used in turbine performance models to calculate the work achievable through adiabatic or isentropic expansion.[47] The isentropic expansion factor (γ) is defined by eq 12. It varies with temperature, air humidity, and the combustion products of the fuel (which stem from the fuel to air ratio in the combustor and the hydrogen to carbon ratio of the fuel). Nonetheless for engineering purposes, γ is frequently treated as a constant based on the properties of dry air at some reference temperature.

$$\gamma = C_{p,exhaust}/C_{v,exhaust} \tag{12}$$

NASA polynomials[48] covering the full temperature range of interest are available for all components of air as well as the combustion products, so $C_p(T)$ can be treated as a known quantity. The other heat capacity term C_v is just a little more complicated. A blending rule analogous to eq 11 could be used but is not necessary. To first order the difference between C_p and C_v is equal to the universal gas constant (R), so C_v follows from C_p. Optionally, R may be scaled by the gas' compressibility factor (Z) or replaced by the value of $(C_p - C_v)_{air}$ at a reference temperature and pressure for which both values are known and applicable to the operating environment of the turbine (up to 40 atm). Engineers may even go so far as to represent this difference for each exhaust gas component by its exact value,[49] which is given by eq 13, where T is temperature, α_T is the coefficient of thermal expansion and β is the isothermal compressibility. This, of course, is only possible because (PV_mT) equation of state models exist for each of the components. Fuel effects enter here through H/C as it influences the proportion of H_2O and CO_2 in the exhaust gas and through LHV as it influences the fuel to air ratio necessary to achieve a mission-point-demanded level of thrust, both of which are easily determined from composition.

$$(C_p - C_v)_T = TV_m \frac{\alpha_T^{\,2}}{\beta} \approx (C_p - C_v)_{ref} \approx ZR \approx R \tag{13}$$

3.4. Other Thermal Properties. The Prandtl number (Pr), defined as the ratio of kinematic viscosity (ν) to thermal diffusivity (α_H), is a significant factor in heat transfer correlations and is represented here by eq 14.[50] The thermal diffusivity is the ratio of thermal conductivity (k) to heat capacity per unit volume (ρC_p), as indicated by eq 15. The kinematic viscosity term is discussed in section 3.5, Fluidity Properties, while the thermal conductivity term is discussed in this section.

$$Pr_{fuel} = \nu_{fuel}/\alpha_{H,fuel} \tag{14}$$

$$\alpha_H = k_{fuel}/C_{p,fuel}\rho_{fuel} \tag{15}$$

$$\alpha_H = \langle \vec{Y} | \vec{\alpha}_H \rangle \tag{16}$$

A direct blending rule for Prandtl number might avoid compounding of uncertainties, but to the best of the authors knowledge, no such blending rule exists. Similarly, the authors are not aware of any published evaluation of a blending rule for thermal diffusivity. eq 16, where $\vec{Y}$ is the mass fraction vector, is proposed here. However, it is unclear whether directly measured, component thermal diffusivity data is significantly more precise than component thermal diffusivity data that is derived from conductivity, density and heat capacity measurements. Applying eq 16 to binary mixtures of isooctane and heptane, we found mean error of 7.43% relative to the archival literature on thermal diffusivity data of hydrocarbon mixtures.[51,52]

Thermal conductivity prediction of liquid mixtures has been the subject of several archival studies, including most recently Rokni et al.[53] and Malatesta and Yang.[54] A prevalent theme in thermal conductivity models for mixtures is to employ a generalized form of a thermal conductivity model for pure materials, where a blending rule is used to generate the inputs. These two studies employed an entropy scaling approach, for which several inputs are required that may not be generally available, including the reduced residual entropy, an equation of state, and a collision integral. Most of the more sophisticated models require the critical temperature, volume and pressure as input to a submodel buried in layers of detail. While there is no questioning the superior accuracy with model evolution beyond the mass fraction weighted average model proposed in 1956,[55] it remains to be seen whether such accuracy is truly worth the cost in terms of computational resources, human labor or outright loss of applicability to complex mixtures that

https://doi.org/10.1021/acs.energyfuels.4c02457
Energy Fuels 2024, 38, 17128−17145

have never been produced. This simple blending rule is expressed here as eq 17.

$$k_{fuel} = \langle \vec{Y} | \vec{k} \rangle \tag{17}$$

Using temperature (only) dependent models published by National Institute of Standards and Technology (NIST),[56] Phoon et al.[90] generated five sets of data with temperature equal to 288, 323, 358, 393, or 428 K, spanning the range of fuel temperature that would potentially be encountered during the normal operation of an aircraft. The standard relative deviation of these data points ranges from a low of 17.3% at 288 K to a high of 19.4% at 428 K with no apparent correlation with carbon number or family. The jet fuel conductivity values reported by Malatesta and Yang[54] are all within the scatter of the neat material conductivity values in this database, hinting that a simple scalar product model may in fact be good enough for engineering purposes despite the decades of development of more elaborate models. Evidence to the contrary, perhaps motivating some of the early work toward the development of elaborate models, includes a fact pointed out by Baroncini et al.[57] that the conductivity of some binary mixtures of polar (and presumably associated) organic molecules does not follow interpolation rationale. We consider such mixtures to be well outside the range of potential aviation fuels, which are comprised of many non-associated species. Considering two articles[58,59] documenting the thermal conductivities of binary mixtures of normal alkanes with other normal alkanes or aromatics, the maximum observed error of the scalar-product blending rule is 2.6%.

3.5. Fluidity Properties. The fuel-dependent factor (Oh') of the Ohnesorge number ($Oh = Oh' L_{char}^{-0.5}$), defined by eq 18, combines three fuel properties that are known to influence atomization of fluids into a single property that is significantly more correlated with important spray characteristics and outcomes such as ignition[60,61] than viscosity, surface tension (σ) or density. To the best of the authors knowledge no one yet has proposed a blending rule for Oh'. Such a rule, to directly calculate Oh' from composition and component Oh' could be convenient, but is unlikely to reduce prediction uncertainty because there is no direct measurement of Oh' to apply to the components separately. In this section the errors associated with the blending rules for viscosity and surface tension are discussed, where emphasis is placed on viscosity because it varies with composition and temperature much more so than density or surface tension and because it also contributes strongly to the Prandtl and Reynolds numbers.

$$Oh' = \nu\sqrt{\rho/\sigma} \tag{18}$$

Hernandez et al.[62] recently compared 30 different blending rules for the viscosity of petroleum-based fuels using 303 measured data points of biodiesel and petroleum/biodiesel binary blends. Nine of the 30 blending rules showed a relative standard error below 5%. The Arrhenius blending rule,[63] represented here by eq 19, was among the most accurate and the most straightforward. Separately, Boehm et al.[36] determined the accuracy of this model by comparing 675 measured and predicted viscosities of simple to complex mixtures of aliphatic and aromatic hydrocarbons in the jet fuel volatility range. eq 19.1 summarizes their accuracy assessment where $\xi(T)$ equals 0.132 at −40 °C and 0.096 at −20 °C. The unity plot they published is reproduced here as Figure 2. It very clearly shows less error with increasing mixture complexity, thereby supporting the presumption expressed by eq 1 (eqs 8.1, 11.1, 19.1, etc.).

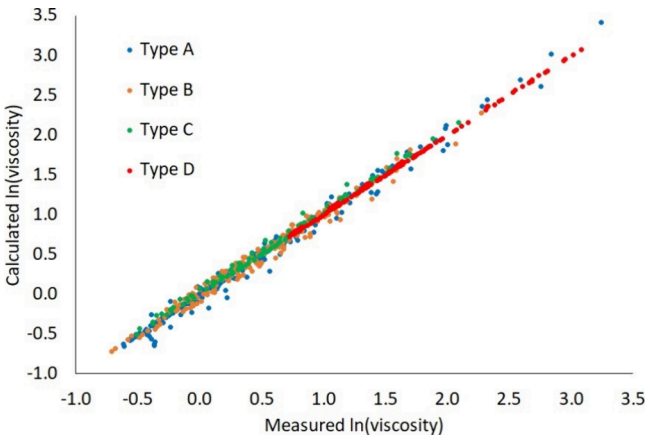

Figure 2. Unity plot for Arrhenius blending rule. Binary mixtures of aliphatic and aromatic hydrocarbons within the jet fuel volatility range. Type A: Both mixture constituents are comprised of a single component. Type B: One mixture constituent is a single component; the other is a 50:50 (by volume) mixture of two components. Type C: One mixture constituent is a single component; the other is a complex mixture. Type D: Both mixture constituents are complex mixtures. The reference viscosity is 1 cSt. This figure was reproduced with permission from ref 36. Copyright 2022 Frontiers.

$$\nu_{fuel} = \langle \vec{X} | \vec{\nu} \rangle \tag{19}$$

$$\sigma = \xi(T)\nu_{fuel}\sqrt{\left(\sum_i x_i^2\right)} \mid x_i \leq 0.5 \tag{19.1}$$

The surface tension at 22 °C of 29 jet-fuel-range molecules extracted from DIPPR database[64] is 18 to 40 mN/m, with a strong dependency on hydrocarbon family that mirrors that of density. The blending rule for mixtures of aliphatic and aromatic hydrocarbons in the jet fuel range, eq 20, is simplified from the general form published in 1986 by Hugill and Van Welsene.[65] The interaction terms are all set to 1 since aviation fuels are non-associated mixtures and the density of the vapor phase is set to 0 since it is much less than the liquid phase density at −10 to 40 °C, corresponding to the reference temperature range for which (lab-ambient-pressure) surface temperature measurements are required by ASTM D4054. This formulation is consistent with earlier expressions of the blending rule dating back to 1929[66] but a detailed, statistical analysis of its error, when applied strictly to mixtures of aliphatic and aromatic hydrocarbons has not been published to the best of our knowledge. There is, however significant, even if anecdotal, evidence[65] that a linear interpolative blending rule for surface tension is reasonable, particularly for these types of mixtures. Using data from Schmidt[67] and Bezerra[68] with a total of 55 sets of data points, this blending rule has a mean absolute error of 1.07 dyn/cm and a mean relative error of −2.85%.

$$\sigma_{fuel}^{0.25} = \langle \vec{X} | \vec{\sigma}^{0.25} \rangle \tag{20}$$

The phase transition from liquid to solid has obvious and severe implications with regard to fluidity, so the freeze point (T_{fp}) is classified here as a fluidity property. Boehm et al.[69] showed that the freeze point of 41 simple to complex mixtures containing *n*-tridecane and/or bicyclohexyl is determined by the concentration of that component along with its phase transition thermal properties; heat of fusion (ΔH_{fus}), entropy

https://doi.org/10.1021/acs.energyfuels.4c02457
Energy Fuels 2024, 38, 17128−17145

of fusion (ΔS_{fus}), freeze point (T_{fp}), and heat capacity ($C_{p,solid}$ and $C_{p,liq}$). It was therefore proposed that the freeze point of fuel is the maximum freeze point of its components, restated here as eq 21, where the subscript, "mix" refers to any mixture of aliphatic and aromatic hydrocarbons having the same mole fraction of component i as the fuel of study. This idea goes back to first principles and illuminates the physics supporting earlier work[70−72] that technically was directed toward understanding the relationship between the freeze point of fuel and normal paraffins concentration and size distribution. In this theory, every fuel component would have a corresponding freeze point predicted by eq 22.

$$T_{fp,fuel} = \max\{T_{fp,mix,i}\} \tag{21}$$

$$T_{fp,mix,i} = \frac{\Delta H_{fus,i} + x_i(C_{p,solid,i} - C_{p,liq,i})(T_{fp,i} - T_{fp,mix,i})}{\Delta S_{fus,i} + x_i(C_{p,solid,i} - C_{p,liq,i})\ln\left(\frac{T_{fp,i}}{T_{fp,mix,i}}\right) + \zeta\Delta S_{mixing}} \tag{22}$$

The inputs to eq 22 pertain to the pure material unless otherwise specified and ζ is a parameter between 0 and 1 that can be tuned for each component, accounting for the difference between the entropy of mixing of an ideal solution and the actual entropy of mixing of the fuel. By default, ζ = 0.25, resulting in a conservative freeze point prediction that could be too high (never too low) by upward 20 °C at low mole fractions where the change in freeze point with concentration is steep. The implication of this conservatism from the perspective of fuel formulation is that a lower-than-truly necessary cap on the concentration of that component would be set. With tuning, the model error reduces to less than 5 °C, where tuning can be accomplished by varying ζ to attain the best fit to freeze point data of prepared binary mixtures containing the subject molecule and some low-freeze solvent such as isooctane. Mixtures containing two or more components that freeze out of solution at nearly the same temperature are the least likely to be well-approximated by eq 22, however the main issue with this model is the sparsity of input data to supply it. The DIPPR database[64] contains the freeze point temperature of approximately 200 molecules in the jet fuel range and just a few of those also have heat or entropy of fusion. Also, the heat capacity terms in eq 15 should be evaluated at the midpoint temperature between the freeze point of the pure component and the freeze point of that component in the solvated state, meaning the liquid state is supercooled. Boehm et al.[69] suggested using the pure-component heat capacity models proposed by Naef[73] with extrapolation to the temperature of interest. For materials with a known freeze point temperature but unknown heat (or entropy) of fusion, Boehm suggested using Walden's rule of thumb estimate for entropy of fusion, which is 56.5 J mol^{-1} K^{-1}.[74] It is not known how much (data input uncertainty) error is introduced into the component freeze point prediction by this approximation. Another issue with eq 22 is that it is difficult to solve for materials with a low entropy of fusion as the denominator flips between positive and negative values during the iteration. Some revision may be necessary to ensure that the first two terms in the denominator never sum to a value less than zero.

The good news is that common sense can be applied to eq 21. There is no need to include any component whose neat freeze point is below −40 °C and there is no need to include any component whose mole fraction is below a threshold value, approximately 5%. A mixture containing mostly high freeze point components (higher than −40 °C), all at very low concentration, may not technically freeze at −40 °C or higher, but its viscosity may be higher than the 12 cSt limit. The freeze point model is a good tool to catch formulations with too much of any one high freeze point component, or to identify a need for freeze point measurements of surrogate mixtures containing the proposed fraction of the at-risk component(s). The viscosity blending rule is a more convenient tool for evaluating fluidity.

Using the data published by Affens et al.[71] as additional evidence supporting the premise behind eqs 21 and 22, the data they provide for the normal alkanes from C12 to C17 can be used to tune eq 22 or serve directly as a prediction curve for any fuel mixture that contains those normal alkanes. As noted by Solash et al.,[70] these are the molecules that are most commonly responsible for the freeze point of fossil, aviation fuels. Similar data sets for all high-freeze-point components of SAF that are not normal alkanes do not yet exist.

3.6. Volatility Properties. Volatility properties consist of vapor pressure as a function of temperature, the distillation curve corresponding to the mass recovered vs temperature resulting from a specified procedure and apparatus at ambient pressure, and the composition of the vapor phase throughout the non-equilibrium transformation between the liquid phase and the vapor phase. From the perspective of fuel formulation design, fuel volatility is all about its vapor pressure. The gas phase composition follows from the vapor pressure and so does the distillation curve, given an accurate model of the still and its operating conditions.

According to Dalton's law, the total pressure is the sum of the partial pressures (p_i) of each component in the gas phase, reproduced here as eq 23. There is no modeling error associated with this blending rule. The estimation of partial pressures of components in real gas mixtures is a topic covered in chemistry education[75,76] and differences between real gases and ideal gases (for which the partial pressure is equal to the component mole fraction times the total pressure of the system, $RT/V_{m,gas}$) can be significant, particularly for dense gases and molecules with unusually strong intermolecular interactions. While the aviation industry stakeholders do indeed care about gas properties at pressures up to approximately 50 atm and temperature up to 750 °C, they also care about understanding potential issues such as cavitation which can be caused by incipient boiling with the fuel delivery system, fuel leakage through valves after stopcock caused by vapor pressure exceeding the valve's cracking pressure, droplet evaporation rate before/during ignition and the accel to idle, and droplet evaporation rate at flight idle and throughout throttle chop transients where the combustor inlet air temperature and pressure are relatively low. At these conditions, the deviation of real gas properties from ideal gas properties is negligible relative to other sources of error in eq 24, which is Raoult's law. In this equation, $P_{vap,i}$ is the vapor pressure of pure component i.

$$P_{tot} = \sum_i p_i \tag{23}$$

$$p_i = x_{liq,i}P_{vap,i} = x_{gas,i}P_{tot} \tag{24}$$

https://doi.org/10.1021/acs.energyfuels.4c02457
Energy Fuels 2024, 38, 17128−17145

In a provocative article published 28 years ago, Hawkes[77] proclaimed that Raoult's law is deceptive. While the tone of that article may be harsh, at least as it applies to mixtures of aliphatic and aromatic hydrocarbons in the jet fuel range, additional experimental data are needed to develop any correction to Raoult's law. Pending this result, eq 24 should be used only when necessary. For example, the gas phase composition of partially evaporated droplets may be required to evaluate the chemical properties of the front end of the distillation.

The distillation curve represents the distribution of boiling points present in a fuel. Typically, distillation curve properties are reported as, T_n where n refers to a volume percent distilled, and T is the temperature at which that amount of fuel has vaporized. There are two common ways to measure distillation curve: standard distillation (ASTM D86) and simulated distillation (ASTM D2887). ASTM D86 is the referee method called out in ASTM D7566 even though it carries more experimental error. ASTM D2887 is a gas chromatography method relating chromatographic elution time with boiling point. Physically the differences in the results are dramatic; D86 is effectively a one theoretical plate separation whereas D2887 can be estimated as infinite theoretical plates. Both methods are required by ASTM D4054.

Distillation curve blending has not been explored in depth. Two distillation curves are controlled by ASTM D4054. The relevant experiments are described in ASTM D2887 and ASTM D86. The ASTM D2887 distillation curves are interpreted from gas chromatographic data. As such, the response from common peaks in each chromatogram can be combined in proportion to their mass fraction, consistent with the mass response of the flame ionization detector. There is no uncertainty introduced by the blending rule, as conservation of mass applies rigorously. However, if the raw data is obscured by reporting, the reported data sets can be partitioned into bins of discrete temperature range(s) and the mass in each bin proportionately summed over all mixture constituents.[78] While conservation of mass is invoked as the rationale for this blending rule, some uncertainty is introduced by the transformation between reported distillation curve points and the assignment of mass into bins. Its efficacy is shared in Figure 3, which is pulled from the work of Yang et al.[78] involving 46 mixtures, 21 points each.

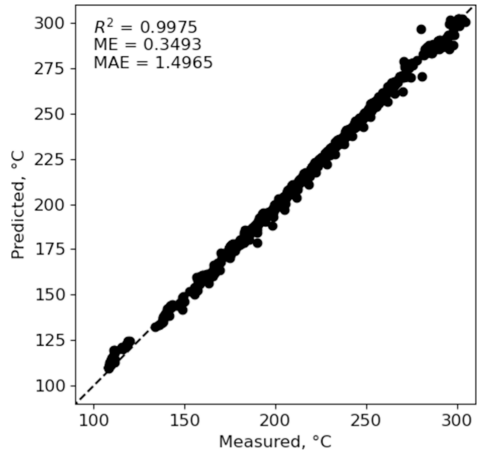

Figure 3. Unity plot for distillation curve (via ASTM D2887) predictions based on components' distillation curves.

For D86 distillation curve prediction, the difficulties in calculating vapor pressure manifest in uncertainty of distillation curve prediction. While an approach like the D2887 method described above may be acceptable, no analysis of its efficacy has been performed. More commonly, the vapor pressure is predicted from eqs 23 and 24 along with some model of the distillation experiment wherein the composition of the liquid phase is updated with each increment of vapor removed from the system. Typically, the total pressure in the experiment is 1 atm so the vapor phase component mole fractions equal their partial pressures.

3.7. Fire Safety Properties. The upper (UFL) and lower (LFL) flammability limits measure, respectively, the maximum and minimum fuel/air ratio required for ignition. In 1891, Le Chatelier[79] used a small set of data to propose a blending rule, represented here by eq 25, for determining the flammability limits of combustible gases commonly used in practical applications. Le Chatelier's rule has since been derived under somewhat differing sets of assumptions;[80−82] the most significant being that adiabatic temperature rise or the heat rise at the flammability limit (FL) is the same for all species. The mole fraction vector in eq 25 includes only the combustible components and the flammability limit refers to either the upper or lower limit. This form of the blending rule is particularly practical because a large amount of single-species fuel component flammability limit data exists within the archival literature,[83−86] data compilations[87] and most Material Safety Data Sheets, to name a few sources. However, the compiled data sources may preferentially report the most conservative measurements.[88]

$$1/FL_{\text{fuel}} = \langle \vec{X} | \overrightarrow{1/FL} \rangle \tag{25}$$

The accuracy of eq 25 is satisfactory when applied to the LFL and offers a respectable guess when applied to the UFL. Coward and Jones[83] reviewed flammability limits for a wide range of flammable gas mixtures and qualitatively described good adherence to Le Chatelier's rule for light hydrocarbons with air. More recently, Liekhus et al.[85] found a mean relative error (MRE) of 8.5% for the LFL of 27 mixtures containing volatile organic compounds and Kondo et al.[84] showed 1.21 and 7.19% MRE for the LFL and UFL, respectively, of 86 mixtures. Beneficial in the context of this work, hydrocarbons are found to be particularly consistent with Le Chatelier's rule, and the predicted flammability limits tend to bracket the experimentally observed limits. Modifications to reduce blending rule error do exist,[82,84,85] but their added complexities render the equations impractical for most applications related to aviation fuel. Lastly, the recent work of Qi et al.[89] contains a comprehensive review of flammability limits, including prediction methods for flammability limit data not found in the other cited works.

Although not represented by eq 25, the limits of flammability also depend on the relative oxygen (or oxidizer) to inert concentration in the mixture as well as the starting temperature of the experiment. Rowley[88] suggests modifications to the models to account for these variations, and also suggests an extension of these concepts to predict the flash point temperature (T_{flash}). While this is an intriguing idea, the incentive to develop a new flashpoint point model is rather low because a number of empirical correlations already exist that appear to be satisfactorily predictive for petroleum distillate fuels and SAF alike. Thorough reviews of these models have

https://doi.org/10.1021/acs.energyfuels.4c02457
Energy Fuels 2024, 38, 17128−17145

been recently published.[90,91] The Wickey model,[92] which is reproduced here as eq 26 was found to be the most consistent, with a global mean absolute error of 1.72 °C.[91] In this empirical model, each flash point is converted to a unitless, flash point index (FPI), the blending rule is applied to the index, and the that result is then converted back into a temperature.

$\mathrm{FPI}_{\mathrm{fuel}} = \langle \vec{v} | \overrightarrow{\mathrm{FPI}} \rangle$ where each component in $\overrightarrow{\mathrm{FPI}}$ is determined as follows:

$$\log_{10}(\mathrm{FPI}) = -6.1188 + 4345.2/(383 - T_{\mathrm{flash}}) \quad (^{\circ}\mathrm{F\ units}) \tag{26}$$

Extension of flammability models to non-standard inlet temperatures, pressures, and "air" compositions is more intriguing because combustors within turbine engines operate over a wide range of inlet temperatures and pressures (and potentially water content—such as some ground-based power plants that are subject to stringent NO_x emission regulations), while afterburners operate with inlet air that is approximately 1000 °C, which is well above the standard reference temperature of 20 °C and they receive vitiated air instead of clean air to oxidize the fuel that is supplied to them. Nonetheless, flammability models extended to non-standard inlet conditions are regarded as out-of-scope for this review.

3.8. Electromagnetic Properties. For non-magnetic materials with no permanent dipole, the dielectric constant, ε_r (also known as relative permittivity), refractive index, n and polarizability (α), are all relatable through simple algebraic expressions written below as eqs 27 and 28, in which N_A is Avogadro's number and ε_0 is the permittivity of free space.[76] A blending rule, can be applied to either polarizability[93,94] or dielectric constant.[94,95] These blending rules are reproduced here as eqs 29 and 30, respectively. Since the "effective" polarizability of a mixture (α_{fuel}) is not directly observable, the accuracy assessment of eq 29 is tied to eq 27. In other words, the dielectric constant of a mixture can be estimated from eq 30 directly or it can be estimated from eq 27 by using the effective polarizability from eq 29 along with a known molar volume as independent variables to determine the dielectric constant. In recent benchmarking against 160 dielectric constant measurements[99] of samples consisting of both simple and complex mixtures of aliphatic and aromatic hydrocarbons within the jet fuel range, Yang et al.[94] found 0.0013 MAE and 0.0003 ME between measured and predicted values of dielectric constants when the fuel dielectric constant was calculated from eqs 27 and 29, and 0.0038 MAE and 0.0037 ME when the dielectric constant was calculated directly from eq 30. While these metrics indicate superior accuracy by using the eqs 27 and 29, Yang et al. emphasize that the accuracy of this approach depends on the concentration of species with non-zero dipole moments and the magnitude of those dipole moments. eq 30, however, is more generally applicable, easier to use and its accuracy is believed to be well represented by the assessment they executed. In contrast, a particularly useful utility of eq 27 is to calculate dielectric constant data for nonpolar fuel constituents based on modeled polarizabilities.[96]

$$\alpha = \left(\frac{3\varepsilon_o}{N_A}\right) V_m \frac{\varepsilon_r - 1}{\varepsilon_r + 2} \tag{27}$$

$$n = \sqrt{\varepsilon_r} \tag{28}$$

$$\alpha_{\mathrm{fuel}} = \langle \vec{X} | \vec{\alpha} \rangle \tag{29}$$

$$\varepsilon_{r,\mathrm{fuel}} = \langle \vec{v} | \vec{\varepsilon}_r \rangle \tag{30}$$

3.9. Chemical Properties. With rare exceptions to be discussed here, the chemical properties of complex mixtures such as fuel do not lend themselves to prediction by simple algebraic models. Rather, chemical kinetic models are needed and excellent work has been published showing that kinetic models of surrogate fuels that match the H/C, Mw, derived cetane number (DCN) and threshold sooting index (TSI) of a corresponding real fuel are able to predict its combustion properties.[17,18] The execution of such a model to predict combustion properties is too computationally intensive to be done within the innermost loop of a fuel composition optimization. That said, algebraically simple blending rules for H/C and Mw, two of the four target properties used for fuel surrogate development, are exactly accurate as discussed in section 3.1, Conservation of Mass. The other two property targets (TSI and DCN) are discussed in this section, before discussion of elastomer/fuel compatibility.

The threshold sooting index, defined by eq 31, was introduced in 1983[97] as a tool to normalize smoke point data from different experiments. A year later, it was leveraged to establish a method to predict the sooting tendency of mixtures based on the sooting tendencies of its constituents[98] which was later validated by several research teams.[99−102] This blending rule is reproduced here as eq 32. A similar blending rule can also be applied to a unified sooting index[103] or a yield sooting index[104] which invoke different raw data to represent sooting tendency. Motivated by a dearth of experimental data to supply the blending rule, Boehm et al.[102] integrated the (linear) TSI blending rule with a linear QSPR (quantitative structure−property relationship) model to estimate $\mathrm{TSI}_{\mathrm{fuel}}$ based on the integrated carbon fragment counts of the fuel, where the blending rule for each carbon fragment is exact, obeying the conservation of mass principle. The standard deviation of that QSPR model was estimated to be 4.5 TSI, slightly less than a more general QSPR model for sooting tendencies of oxygenated fuels that was published a few months earlier.[103] In contrast, the standard deviation of the uncertainty ascribed to the blending rule, eq 32 was estimated to be less than one index point. On the other side, the real variation between isomers within the same concentration bin, as defined by a stenciled region with a chromatograph from a GC × GC−FID experiment is much, much larger than one index point because branching has a large impact on TSI but no impact at all on molecular weight.

$$Sp_{\mathrm{fuel}} = b\mathrm{Mw}_{\mathrm{fuel}}/(\mathrm{TSI}_{\mathrm{fuel}} - a) \tag{31}$$

a and b are calibration coefficients for a specific operator and experimental arrangement and are calibrated by the smoke points of methylcyclohexane and 1-methyl naphthalene.

$$\mathrm{TSI}_{\mathrm{fuel}} = \langle \vec{X} | \overrightarrow{\mathrm{TSI}} \rangle \tag{32}$$

Historically, the cetane number, or the propensity of a fuel to autoignite under reference conditions, was measured in a CFR engine per ASTM D613. Over the last several decades the derived cetane number or DCN has gained favor in the combustion field for its ease of use, repeatability, modest footprint in the lab, and reproducibility across laboratories. Subsequent to its widespread use, the DCN has been found to correlate to aviation relevant metrics. The derived cetane

https://doi.org/10.1021/acs.energyfuels.4c02457
Energy Fuels 2024, 38, 17128−17145

number is calculated from the ignition delay according to the procedures and equipment described in ASTM.[105] DCN and the initial metric, cetane number, have long been used as metrics to characterize ignition quality of fuels used in compression-ignition engines. It has also been shown[106] to be strongly correlated with lean blow out of continuous flow combustors. Moreover, its correlation with gas-phase auto-ignition delay time is strong over a range of temperature, pressure and equivalence ratio conditions.[107,108] Regression models leveraging input from FTIR analysis of drop-size fuel samples have been shown to predict DCN of validation set samples with an RMS error of 1−2 index points.[109−111] Similar efforts have also used liquid phase IR absorption to predict DCN using linear and nonlinear models with similar accuracy.[23] Aside from the drawback of needing at least a drop of sample fuel to get the FTIR spectral feature inputs, the regression models cannot predict the DCN of partially vaporized fuel because the FTIR spectrum may vary significantly from one distillation fraction to another and to the best of the authors knowledge there is not yet a standardized experimental method to attain FTIR data of the vapor fraction of two-phase samples, nor is there a processing methodology to relate such data to distillation fractions.

The extent of vaporization and the mixedness of the vapor phase of the fuel inside a jet-engine combustor, leading up to forced ignition, lean blow out, autoignition forward of the intended flame front and even normal operating conditions for that matter are difficult to model accurately with computational fluid dynamics, or any other approach. To assess fuel effects on combustion metrics such as these, complex chemical kinetic models are required, but the human and machine labor involved to do this is extensive, requiring days or weeks to complete each fuel assessment on each combustion metric. At low fuel readiness level, such a drain on resources is impractical. A more tractable approach, relating the vapor fraction of the fuel throughout the vaporization transient to its DCN, in combination with other 1D models of the combusting system, affords stakeholders an early indication of whether the compositional differences between a SAF concept product and a conventional jet fuel will have a deleterious effect on the combustion metric of study. eq 33 is one model for making this connection.

$$\mathrm{DCN}_{\mathrm{fuel(gas)}} = \langle \vec{c} | \overrightarrow{\mathrm{DCN}} \rangle \tag{33}$$

The maximum uncertainty associated with eq 33 is large; see Figure 4. The model itself has a mean absolute relative error of 2.9%. Moreover, when the blending rule is applied to partially vaporized fuel, the gas phase composition uncertainty can also be significant, as discussed in section 3.6, Volatility Properties. Additionally, the uncertainty regarding the property vector input is particularly substantial for a DCN blending rule. The database of measured pure component DCN values is so sparse that other models[1,23,110,112,18,114] must be used to populate $\overrightarrow{\mathrm{DCN}}$, which leads to significant database uncertainty. Moreover, the undetermined isomer uncertainty is particularly large for DCN because this property is known[28] to be strongly impacted by branching, while the GC × GC stencil regions encompass all molecules having the same number of carbons that belong to the same hydrocarbon family.

The material compatibility of fuel is primarily concerned with the intercalation of certain fuel constituents into elastomeric materials. Effects of the fuel/elastomer interaction

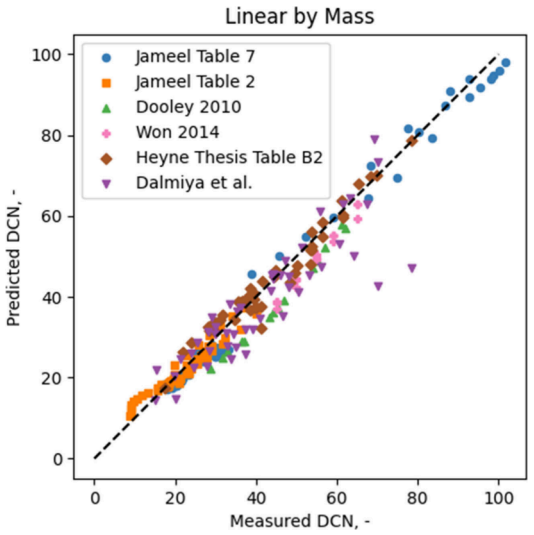

Figure 4. Unity plot showing DCN blending rule error. Data sources: refs 113−117.

are commonly quantified with volume swell measurements during an O-ring soak test. These tests require days or even weeks of soak time to complete and the results vary between manufacturing batches of O-rings.[118−122] The testing complications present a challenge to the establishment of material compatibility requirements in the fuel approval process, as a comprehensive database of standard component swell values is sparse and therefore limiting for both proposed fuel evaluations and scientific studies aimed at predictive blending rules. Informed by the available literature, Kosir et al.[123] proposed the linear volumetric blending rule found in eq 34.

$$Sw_{\mathrm{fuel}} = \langle \vec{v} | \overrightarrow{Sw} \rangle \tag{34}$$

This rule was validated by Faulhaber et al.[118] for binary blends of 4 single dopant molecules from different hydrocarbon classes at 3−40 vol % in a SAF comprised entirely of aliphatic hydrocarbons. These 24 results, along with 28 additional swell measurements of binary and ternary mixtures, are found in Figure 5. For this demonstration, single-species swell was

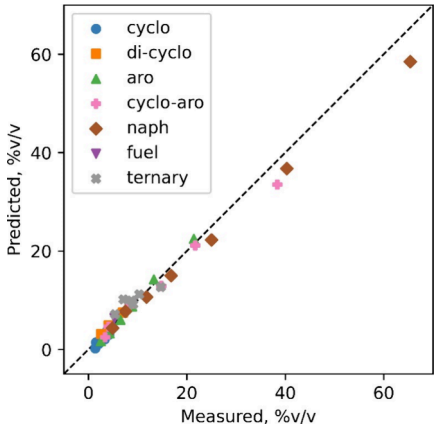

Figure 5. Unity plot showing O-ring volume swell blending error for 42 mixtures measured using optical dilatometry method of Faulhaber et al.[118] The legend indicates hydrocarbon type of species doped in SPK, except for "fuel" and "ternary", which indicate fuel−fuel blends and single-species/single-species/SPK blends, respectively.

https://doi.org/10.1021/acs.energyfuels.4c02457
Energy Fuels 2024, 38, 17128−17145

quantified using measurements of each molecule doped at 8 vol % in synthetic paraffinic kerosene (SPK) and extrapolated to 100 vol %. This was done to avoid O-ring test sample degradation that can occur during soak tests using single species aromatic solvents. Volume swell of fuels, on the other hand, were simply measured at 100 vol %.

The MAE for these 52 total measurements is 1.23% (v/v). Comparing this to the O-ring swell experience range for conventional jet fuel found with this experimental method (8.3−17.1%, v/v), the total uncertainty ranges between 7 and 15% of the swell expected for elastomer compatibility. However, it is expected that experimental error comprises a large portion of this uncertainty. Further O-ring swell measurement campaigns will afford more comprehensive validation of this rule and associated experimental error, including investigation of potential interaction effects in complex mixtures and the impact of trace amounts of heteroatoms.[119,121,124,125] A key part of these continuing efforts will be the collection of single component swell data to construct a model based on observed relationships between elastomer swell and other molecular properties or structural identifiers to predict the swell of compounds that are not readily available for measurement, building on the works of Graham et al.[121] and Landera et al.[30] whose respective models relate elastomer swell with Hansen solubility parameters.[11,126]

4. CHALLENGES TO PROPERTY PREDICTIONS FOR JET FUEL DESIGN AND QUALIFICATION

Looking forward, there are five themes poised for advancements. These include (1) quantification of prediction uncertainty category one (regression) and three (hybrid) models, (2) dissemination of probabilistic property prediction software, (3) integrating category one (regression) with category two (blending rules) models to refine the composition characterization, (4) addition hybridization opportunities to reduce model uncertainty, and (5) prediction impurity-sensitive properties such as those listed in column D of Table 1. A brief paragraph is devoted to each of these themes.

Throughout the sciences, there has been widespread application of machine learning to develop interpolative relationships between different characteristics of the population. Few of the articles that showcase these models address potential overfitting errors or uncertainties arising from epistemic errors (population is not representative of the sample for which a property estimate is desired) or heteroscedastic errors arising from non-uniformity of variances over the range of independent variables. Two notable exceptions include the works of Oh et al.[21] and Hall et al.[13] Tools that are excellent at finding and leveraging strong correlations between features that are distributed throughout a large population[127] are not necessarily applicable to problems where the variation in the uncharacterized population (desired prediction) may be substantially different from the variation observed in the characterized population (training, validation and test sets). To the point, more education is needed around the application limits of regression-based models.

Frequently, the results of machine-learning models are published, absent disclosure of the model itself. While it may be reasonable to presume that independent researchers could acquire the same data used in the original research and follow the same prescription to derive a similar, interpolation scheme, this presumption is unprovable without definition of the original model. Demotivating the creation of such models or models for which uncertainty quantification is incomplete could be accomplished by making the models that do include comprehensive uncertainty quantification more readily available. This review assists to that end. Additionally, the revision-controlled software that utilizes the blending rules discussed in this review and makes the uncertainty determinations could be made available online along with the NIST database upon which it relies.

One potential application of machine-learning models which has not been explored in detail is an integration with blending rules; tier-alpha models,[10] where both models use species concentration data from a GC × GC experiment as input. Perhaps the coefficients of the regressed model could serve as probabilistic constraints to be imposed on the selection of isomers used to represent a particular hydrocarbon bin in the tier-alpha model framework. The isomeric population distributions that bring the tier-alpha-like[10] prediction into alignment with the regressed model interpolation for one property (or set of properties) may be used to narrow the undetermined isomer contribution to the tier-alpha-like predictions of other properties.

There are, in fact, many opportunities to integrate different modeling approaches and to maximize their utilization of disparate data streams to reduce overall prediction uncertainty. Simple examples of this notion include utilization of *C#*, *H#* and total aromatics content to bound the total concentration of cycloalkanes. It is more complicated to simultaneously leverage GC × GC data, spectroscopic data, and physiochemical properties. One tactic would be to let any piece of data serve as a constraint within the tier-alpha framework. For example, NMR data could provide information on chain branching, which could, in principle, be imposed on the isomeric selections within the tier-alpha framework. Another possibility would be to create a model integration method whereby the probabilistic predictions of different modeling approaches are encouraged to inform one another; resulting in an integrated property prediction with a narrower uncertainty band.

While each of the four potential advances which have been noted so far are interesting in the own right, the biggest gap in SAF property predictions has to do with the properties listed in column D of Table 1. These properties are believed to be strongly influenced by impurities and other components that may be present in fuel at very low concentration; perhaps even below the detection limit of analytical methods that focus on qualification and quantification of individual components within a mixture. A review of existing models to estimate these properties is needed, and we believe such a review will reveal significant gaps to be filled by future research and development.

5. CONCLUSION

A summary of each blending rule assessment is provided in Table 2. Raoult's law, for vapor pressure is left off the list because its accuracy, when applied to mixtures of many components, is not known. This is the most impactful gap within our collective knowledge of model accuracy because it has a direct bearing on the ASTM D86 distillation curve (e.g., T_{10}, T_{50}, and T_{90}) and the gas phase concentration. Overall, thirty-two different fuel properties can be estimated from simple algebraic models involving 16 scalar products, one simple equation of state model, and well-known property-property relationships. Six of the base properties including

https://doi.org/10.1021/acs.energyfuels.4c02457
Energy Fuels 2024, 38, 17128−17145

Table 2. Summary of Blending Rule Accuracy Assessments

property	blending rule uncertainty	number of data points used	source
carbon number	0	CoM[a]	
hydrogen number	0	CoM	
density	MARE 0.24 (%)	675	36
lower heating value	ME 0.15 (kJ/kg)	27	40
liquid heat capacity	MRE 0.9 (%)	81	43
thermal conductivity	max 2.6 (%)	22	58 and 59
kinematic viscosity	MARE 3.9 (%)	675	36
surface tension	MRE −2.85 (%)	55	67 and 68
freeze point	max 20 (°C)	41	69
distillation curve (ASTM D2887)	MAE 1.5 (°C)	966	78
lower flammability limit	MRE 1.3 (%)	86	84
flash point	MAE 1.72 (°C)	153	91
dielectric constant	MAE 0.0038	200	94
threshold sooting index	MAE <2	confounded	102
derived cetane number	MARE 2.9 (%)	278−100	113, 115−117, and 128
elastomer swell	MAE 1.23 (%, v/v)	52	118

[a]CoM = conservation of mass.

carbon number, hydrogen number, lower heating value, heat capacity of the gas phase, dielectric constant and the distillation curve as defined by ASTM D2887 are predicted essentially exactly by the scalar product blending rule since intermolecular forces have no substantive effect on these properties. Another six base properties can be predicted from composition and component data with model uncertainty that is small relative to other sources of uncertainty. These properties include density, liquid-phase heat capacity, threshold sooting index, elastomer seal swell, flash point, and the lower flammability limit. Three properties that depend significantly on intermolecular forces include kinematic viscosity, surface tension and thermal conductivity. Even these properties are reasonably well approximated by a scalar-product blending rule, having prediction uncertainties less than 4% when applied exclusively to mixtures of aliphatic and/or aromatic hydrocarbons. The freeze point can also be predicted well (<5 °C) from composition provided there is also a collection of reference data for each high-freeze-point component as a function of concentration in a reference, hydrocarbon solvent. Absent the reference data, however, freeze point predictions can be too high by as much as 20 °C. The derived cetane number, which intuitively should be modeled through detailed kinetics is well approximated by a simple blending rule for many mixtures. However, the scalar-product blending rule applied to some mixtures does result in a DCN prediction error greater than 20%.

AUTHOR INFORMATION

Corresponding Author

Joshua S. Heyne − *Bioproduct Sciences and Engineering Laboratory, School of Engineering and Applied Science, Washington State University, Richland, Washington 99354, United States; Energy Processes and Materials Division, Energy and Environment Directorate, Pacific Northwest National Laboratory, Richland, Washington 99352, United States;* orcid.org/0000-0002-1782-9056; Email: joshua.heyne@wsu.edu

Authors

Randall C. Boehm − *Bioproduct Sciences and Engineering Laboratory, School of Engineering and Applied Science, Washington State University, Richland, Washington 99354, United States;* orcid.org/0000-0003-2983-1337

Zhibin Yang − *Bioproduct Sciences and Engineering Laboratory, School of Engineering and Applied Science, Washington State University, Richland, Washington 99354, United States*

David C. Bell − *Bioproduct Sciences and Engineering Laboratory, School of Engineering and Applied Science, Washington State University, Richland, Washington 99354, United States;* orcid.org/0000-0002-7463-0035

Conor Faulhaber − *Bioproduct Sciences and Engineering Laboratory, School of Engineering and Applied Science, Washington State University, Richland, Washington 99354, United States;* orcid.org/0009-0003-5634-0864

Eric Mayhew − *Mechanical Sciences Division, DEVCOM Army Research Laboratory, Aberdeen Proving Ground, Maryland 21005, United States;* orcid.org/0000-0003-2063-4089

Uwe Bauder − *DLR Germany, German Aerospace Center (DLR), Institute of Combustion Technology, 70569 Stuttgart, Germany*

Georg Eckel − *DLR Germany, German Aerospace Center (DLR), Institute of Combustion Technology, 70569 Stuttgart, Germany*

Complete contact information is available at: https://pubs.acs.org/10.1021/acs.energyfuels.4c02457

Notes

The authors declare no competing financial interest.

Biographies

Randall C. Boehm has 24 years of experience advising on fuel effects in combustion systems. As a key contributor to the CRATCAF program for the US Air Force, he helped develop SAF evaluation guidelines in ASTM D4054. He led phase 2 of CRATCAF, resulting in a referee combustion rig that remains a standard today. Dr. Boehm's leadership in combustion research has significantly advanced the understanding of fuel property variation on engine performance.

Zhibin Yang, a doctoral candidate at Washington State University, published his first journal article on surrogate fuels in 2020 after earning his master's degree from the University of Dayton. He has co-authored 10 studies focused on aviation fuel properties and sustainable aviation fuel (SAF) production. His research centers on predictive models for fuel property evaluation, contributing to the advancement of SAF technologies.

David C. Bell, a doctoral candidate at Washington State University, specializes in aviation fuel characterization. He earned his master's degree from the University of Dayton in 2017 and published his first lead-author journal article on noise statistics in 2022. Bell's research includes five key publications, supported by industry experience at GE Aviation (2018−2020). His work advances the identification and assessment of fuel components.

Conor Faulhaber, a second-year Ph.D. student at Washington State University, focuses on jet fuel contaminants and thermal stability. Supported by Alaska Airlines as a graduate fellow and the WSU−PNNL Distinguished Graduate Research Program, he investigates

https://doi.org/10.1021/acs.energyfuels.4c02457
Energy Fuels 2024, 38, 17128−17145

nitrogen-containing compounds in aviation fuels. He holds a B.S. degree in mechanical and aerospace engineering from the University of Dayton, with research experience in O-ring compatibility with sustainable aviation fuels.

Eric Mayhew is an aerospace engineer at DEVCOM Army Research Laboratory, specializing in ignition for internal combustion engines. As a technical area lead for the VICTOR ERP, he directs research on how fuel composition impacts ignition in compression-ignition and gas turbine engines. Dr. Mayhew joined ARL in 2018 after earning his Ph.D. degree in mechanical engineering from the University of Illinois at Urbana−Champaign. His research emphasizes the link between fuel property variation on each phase of the spray combustion process.

Uwe Bauder, an aerospace engineer, leads the Future Refineries team at the German Aerospace Center (DLR) and the SimFuel platform for fuel assessment and optimization. He coordinates DLR's prescreening of novel jet fuels. With a Ph.D. degree from the University of Stuttgart (2015), he joined DLR in 2016. Dr. Bauder has authored over 30 publications on aviation fuel prescreening, optimization, and climate impact. He received NASA's 2019 Group Achievement Award for ND-MAX.

Georg Eckel is the deputy head of Multiphase Flows and Alternative Fuels at DLR and leads the Aviation Fuel Impact Team. He focuses on maximizing SAF benefits and guiding sustainable aviation transitions. Dr. Eckel, part of an EU advisory group on fuel specifications and non-CO_2 impacts, coordinates DLR's activities with the EU and UK SAF Clearing Houses. He earned his Ph.D. degree from the University of Stuttgart in 2018 and has authored 16 aerospace-related articles.

Joshua S. Heyne is the co-director of the WSU−PNNL Bioproducts Institute, director of the Bioproducts, Sciences, and Engineering Laboratory at WSU Tri-Cities, a Battelle Distinguished Professor, and an associate professor of mechanical engineering. He earned his Ph.D. degree from Princeton University in 2014. His research focuses on sustainable aviation fuel (SAF) technologies, including SAF qualification and chemical composition analysis to ensure safety and environmental benefits. He has reviewed over 300 SAF samples from more than 37 institutions globally.

■ ACKNOWLEDGMENTS

The authors Boehm, Yang, Bell, Faulhaber, and Heyne acknowledge funding from the U.S. Federal Aviation Administration Office of Environment and Energy through ASCENT, the FAA Center of Excellence for Alternative Jet Fuels and the Environment, Project 65 through FAA Award 13-CAJFE-WASU-035 (PI: Dr. Joshua S. Heyne) under the supervision of Dr. Anna Oldani and Ana Gabrielian. Any opinions, findings, conclusions, or recommendations expressed in this material are those of the authors and do not necessarily reflect the views of the FAA or other sponsors. The authors Eckel and Bauder acknowledge funding from the DLR internal project Neofuels. This work was done under the auspices of the WSU−PNNL Bioproducts Institute, which is a joint research collaboration of Washington State University and the U.S. Department of Energy's Pacific Northwest National Laboratory.

■ REFERENCES

(1) Goldner, W.; Bredlau, J.; Brown, N.; Haq, Z.; Brown, C.; Galperin, D.; Craig, K.; Csonka, S.; Fitzgerald, J.; Hileman, J.; et al. *SAF Grand Challenge Roadmap Flight Plan for Sustainable Aviation Fuel*; United States Department of Energy: Washington, D.C., 2022; https://www.energy.gov/sites/default/files/2022-09/beto-saf-gc-roadmap-report-sept-2022.pdf (accessed May 22, 2024).

(2) United States Environmental Protection Agency (U.S. EPA). *RINs Generated Transactions*; U.S. EPA: Washington, D.C., 2024; https://www.epa.gov/fuels-registration-reporting-and-compliance-help/rins-generated-transactions (accessed May 22, 2024).

(3) Commercial Aviation Alternative Fuels Initiative (CAAFI). *U.S. SAF Production Potential*; CAAFI: Washington, D.C., 2024; https://www.caafi.org/focus_areas/docs/US_SAF_Production_Potential_March2024.pdf (accessed May 22, 2024).

(4) International Energy Agency (IEA). *Renewables 2021*; IEA: Paris, France, 2021.

(5) Heyne, J.; Rauch, B.; Le Clercq, P.; Colket, M. Sustainable Aviation Fuel Prescreening Tools and Procedures. *Fuel* **2021**, *290*, No. 120004.

(6) Martin, D.; Wilkins, P. *Petroleum Quality Information System (PQIS) 2011 Annual Report*; Defense Technical Information Center: Fort Belvoir, VA, 2011.

(7) The International Civil Aviation Organization (ICAO). *ICAO Global Framework for Aviation Alternative Fuels: Conversion Processes*; ICAO: Montreal, Canada, 2024; https://www.icao.int/environmental-protection/GFAAF/Pages/Conversion-processes.aspx (accessed May 22, 2024).

(8) Heyne, J.; Bell, D.; Feldhausen, J.; Yang, Z.; Boehm, R. Towards Fuel Composition and Properties from Two-Dimensional Gas Chromatography with Flame Ionization and Vacuum Ultraviolet Spectroscopy. *Fuel* **2022**, *312*, No. 122709.

(9) Feldhausen, J.; Bell, D. C.; Yang, Z.; Faulhaber, C.; Boehm, R.; Heyne, J. Synthetic Aromatic Kerosene Property Prediction Improvements with Isomer Specific Characterization via GC × GC and Vacuum Ultraviolet Spectroscopy. *Fuel* **2022**, *326*, No. 125002.

(10) Yang, Z.; Kosir, S.; Stachler, R.; Shafer, L.; Anderson, C.; Heyne, J. S. A GC × GC Tier α Combustor Operability Prescreening Method for Sustainable Aviation Fuel Candidates. *Fuel* **2021**, *292*, No. 120345.

(11) Bell, D.; Heyne, J. S.; August, E.; Won, S. H.; Dryer, F. L.; Haas, F. M.; Dooley, S. On the Development of General Surrogate Composition Calculations for Chemical and Physical Properties. *Proceedings of the 55th AIAA Aerospace Sciences Meeting*; Grapevine, TX, Jan 9−13, 2017; AIAA 2017-0609, DOI: 10.2514/6.2017-0609.

(12) Flora, G.; Kosir, S.; Behnke, L.; Stachler, R.; Heyne, J.; Zabarnick, S.; Gupta, M. Properties Calculator and Optimization for Drop-in Alternative Jet Fuel Blends. *Proceedings of the AIAA Scitech 2019 Forum*; San Diego, CA, Jan 7−11, 2019; AIAA 2019-2368, DOI: 10.2514/6.2019-2368.

(13) Hall, C.; Rauch, B.; Bauder, U.; Le Clercq, P.; Aigner, M. Predictive Capability Assessment of Probabilistic Machine Learning Models for Density Prediction of Conventional and Synthetic Jet Fuels. *Energy Fuels* **2021**, *35* (3), 2520−2530.

(14) Yang, Z.; Boehm, R. C.; Bell, D. C.; Heyne, J. S. Maximizing Sustainable aviation fuel usage through optimization of distillation cut points and blending. *Fuel* **2023**, *353*, 129136.

(15) Miller, J. H.; Tifft, S. M.; Wiatrowski, M. R.; Benavides, P. T.; Huq, N. A.; Christensen, E. D.; Alleman, T.; Hays, C.; Luecke, J.; Kneucker, C. M.; Haugen, S. J.; Sànchez i Nogué, V.; Karp, E. M.; Hawkins, T. R.; Singh, A.; Vardon, D. R. Screening and evaluation of biomass upgrading strategies for sustainable transportation fuel production with biomass-derived volatile fatty acids. *iScience* **2022**, *25*, No. 105384.

(16) Boehm, R. C.; Faulhaber, C.; Behnke, L.; Heyne, J. The Effect of Theoretical SAF Composition on Calculated Engine and Aircraft Efficiency. *Fuel* **2024**, *371*, No. 132049.

(17) Won, S. H.; Haas, F. M.; Dooley, S.; Edwards, T.; Dryer, F. L. Reconstruction of Chemical Structure of Real Fuel by Surrogate Formulation Based upon Combustion Property Targets. *Combust. Flame* **2017**, *183*, 39−49.

(18) Kang, D.; Kim, D.; Kalaskar, V.; Boehman, A.; Violi, A. Experimental Characterization of Jet Fuels under Engine Relevant

Conditions − Part 2: Insights on Optimization Approach for Surrogate Formulation. *Fuel* **2019**, *239*, 1405−1416.
(19) Caceres-Martinez, L. E.; Kilaz, G. Kinematic Viscosity Prediction of Jet Fuels and Alternative Blending Components via Comprehensive Two-dimensional Gas Chromatography, Partial Least Squares, and Yeo-Johnson Transformation. *J. Sep. Sci.* **2024**, *47* (5), No. 2300816.
(20) Vozka, P.; Kilaz, G. Determination of Jet Fuel System Icing Inhibitor by GC × GC−FID. *Talanta* **2020**, *218*, No. 121146.
(21) Oh, J.-H.; Oldani, A.; Solecki, A.; Lee, T. Learning to Predict Sustainable Aviation Fuel Properties: A Deep Uncertainty Quantification Viewpoint. *Fuel* **2024**, *356*, No. 129508.
(22) Berrier, K. L.; Freye, C. E.; Billingsley, M. C.; Synovec, R. E. Predictive Modeling of Aerospace Fuel Properties Using Comprehensive Two-Dimensional Gas Chromatography with Time-Of-Flight Mass Spectrometry and Partial Least Squares Analysis. *Energy Fuels* **2020**, *34* (4), 4084−4094.
(23) Dalmiya, A.; Sheyyab, M.; Mehta, J. M.; Brezinsky, K.; Lynch, P. T. Derived Cetane Number Prediction of Jet Fuels and Their Functional Group Surrogates Using Liquid Phase Infrared Absorption. *Proc. Combust. Inst.* **2023**, *39* (1), 1495−1504.
(24) Kehimkar, B.; Hoggard, J. C.; Marney, L. C.; Billingsley, M. C.; Fraga, C. G.; Bruno, T. J.; Synovec, R. E. Correlation of Rocket Propulsion Fuel Properties with Chemical Composition Using Comprehensive Two-Dimensional Gas Chromatography with Time-of-Flight Mass Spectrometry Followed by Partial Least Squares Regression Analysis. *J. Chromatogr. A* **2014**, *1327*, 132−140.
(25) Mehta, J. M.; Lynch, P. T.; Mayhew, E. K.; Brezinsky, K. Evaluation of Chemical Functional Group Composition of Jet Fuels Using Two-Dimensional Gas Chromatography. *Energy Fuels* **2023**, *37* (3), 2294−2306.
(26) Hall, C.; Creton, B.; Rauch, B.; Bauder, U.; Aigner, M. Probabilistic Mean Quantitative Structure−Property Relationship Modeling of Jet Fuel Properties. *Energy Fuels* **2022**, *36* (1), 463−479.
(27) Vozka, P.; Kilaz, G. A Review of Aviation Turbine Fuel Chemical Composition-Property Relations. *Fuel* **2020**, *268*, No. 117391.
(28) Hall, C.; Bell, D. C.; Feldhausen, J.; Rauch, B.; Heyne, J. Quantifying Isomeric Effects: A Key Factor in Aviation Fuel Assessment and Design. *Fuel* **2024**, *357*, 129912.
(29) Pan, Q.; Fan, X.; Li, J. Automatic Creation of Molecular Substructures for Accurate Estimation of Pure Component Properties Using Connectivity Matrices. *Chem. Eng. Sci.* **2023**, *265*, No. 118214.
(30) Landera, A.; Bambha, R. P.; Hao, N.; Desai, S. P.; Moore, C. M.; Sutton, A. D.; George, A. Building Structure−Property Relationships of Cycloalkanes in Support of Their Use in Sustainable Aviation Fuels. *Front. Energy Res.* **2022**, *9*, 771697.
(31) Watanasiri, S.; Paulechka, E.; Iisa, K.; Christensen, E.; Muzny, C.; Dutta, A. Prediction of Sustainable Aviation Fuel Properties for Liquid Hydrocarbons from Hydrotreating Biomass Catalytic Fast Pyrolysis Derived Organic Intermediates. *Sustainable Energy Fuels* **2023**, *7*, 2413−2427.
(32) ASTM International. *ASTM D8396, Standard Test Method for Group Types Quantification of Hydrocarbons in Hydrocarbon Liquids with a Boiling Point between 36 and 343 °C by Flow Modulated GC × GC−FID*; ASTM International: West Conshohocken, PA, 2022; pp 1−25, DOI: 10.1520/D8396-22.
(33) Johnson, K.; Loegel, T.; Metz, A.; Wrzesinski, P.; Shafer, L.; Striebich, R.; West, Z. Method for Detailed Hydrocarbon Analysis of Middle Distillate Fuels by Two-Dimensional Gas Chromatography. *NAVAIR Public Release* **2020**, 2020−361.
(34) Schofield, K. The Enigmatic Mechanism of the Flame Ionization Detector: Its Overlooked Implications for Fossil Fuel Combustion Modeling. *Prog. Energy Combust. Sci.* **2008**, *34* (3), 330−350.
(35) Bell, D. C.; Feldhausen, J.; Spieles, A. J.; Boehm, R. C.; Heyne, J. S. Limits of Identification Using VUV Spectroscopy Applied to C8H18 Isomers Isolated by GC × GC. *Talanta* **2023**, *258*, No. 124451.
(36) Boehm, R. C.; Hauck, F.; Yang, Z.; Wanstall, C. T.; Heyne, J. S. Error Quantification of the Arrhenius Blending Rule for Viscosity of Hydrocarbon Mixtures. *Front. Energy Res.* **2022**, *10*, 1074699.
(37) Sanghvi, M. K. D.; Kay, W. B. Volume Changes on Mixing in the Cyclohexane-n-Heptane-Benzene System. *Chem. Eng. Sci.* **1956**, *6* (1), 10−25.
(38) Vozka, P.; Modereger, B. A.; Park, A. C.; Zhang, W. T. J.; Trice, R. W.; Kenttämaa, H. I.; Kilaz, G. Jet Fuel Density via GC × GC−FID. *Fuel* **2019**, *235*, 1052−1060.
(39) Nabipour, N.; Daneshfar, R.; Rezvanjou, O.; Mohammadi-Khanaposhtani, M.; Baghban, A.; Xiong, Q.; Li, L. K. B.; Habibzadeh, S.; Doranehgard, M. H. Estimating Biofuel Density via a Soft Computing Approach Based on Intermolecular Interactions. *Renewable Energy* **2020**, *152*, 1086−1098.
(40) Lundberg, G. W. Thermodynamics of Solutions XI. Heats of Mixing of Hydrocarbons. *J. Chem. Eng. Data* **1964**, *9* (2), 193−198.
(41) Boehm, R. C.; Yang, Z.; Bell, D. C.; Feldhausen, J.; Heyne, J. S. Lower Heating Value of Jet Fuel from Hydrocarbon Class Concentration Data and Thermo-Chemical Reference Data: An Uncertainty Quantification. *Fuel* **2022**, *311*, 122542.
(42) Fortier, J. L.; Benson, G. C. Heat Capacities of Some Binary Aromatic Hydrocarbon Mixtures Containing Benzene or Toluene. *J. Chem. Eng. Data* **1979**, *24* (1), 34−37.
(43) Sharma, V. K.; Malik, S.; Solanki, S. Thermodynamic Studies of Molecular Interactions in Mixtures Containing Tetrahydropyran, 1,4-Dioxane, and Cyclic Ketones. *J. Chem. Eng. Data* **2017**, *62* (2), 623−632.
(44) Malik, S.; Gupta, H.; Sharma, V. K. Topological Investigation of Ternary Mixtures: Excess Heat Capacities. *J. Mol. Liq.* **2017**, *233*, 319−325.
(45) Jamieson, D. T.; Cartwright, G. *NEL Report No. 648: Properties of Binary Liquid Mixtures: Heat Capacity*; The National Archives: East Kiibride, U.K., 1978.
(46) Teja, A. S. Simple Method for the Calculation of Heat Capacities of Liquid Mixtures. *J. Chem. Eng. Data* **1983**, *28* (1), 83−85.
(47) Hall, N. *Isentropic Compression*; NASA Glenn Research Center: Cleveland, OH, 2023; https://www.grc.nasa.gov/www/k-12/airplane/compexp.html (accessed Oct 8, 2023).
(48) McBride, B. J.; Zehe, M. J.; Gordon, S. *NASA Glenn Coefficients for Calculating Thermodynamic Properties of Individual Species*; NASA Glenn Research Center: Cleveland, OH, 2002.
(49) BYJU. *CP−CV for Non-Ideal Gases*; BYJU: Bangalore, India, 2023; https://byjus.com/chemistry/cp-cv-for-non-ideal-gases/ (accessed Oct 8, 2023).
(50) Bergman, T. L.; Lavine, A. S.; Incropera, F. P.; Dewitt, D. P. *Fundamental of Heat and Mass Transfer*, 7th ed.; John Wiley & Sons: Hoboken, NJ, 2011.
(51) Isidro-Ojeda, M. A.; Calderón, A.; Marín, E. Thermal Diffusivity of Heptane-Isooctane Mixtures. *Thermochim. Acta* **2020**, *689*, No. 178616.
(52) Bedoya, A.; Alvarado, S.; Calderón, A.; Marín, E. Thermal Transport Properties of Heptane-Isooctane Mixtures. *Thermochim. Acta* **2018**, *666*, 190−196.
(53) Rokni, H. B.; Moore, J. D.; Gupta, A.; McHugh, M. A.; Mallepally, R. R.; Gavaises, M. General Method for Prediction of Thermal Conductivity for Well-Characterized Hydrocarbon Mixtures and Fuels up to Extreme Conditions Using Entropy Scaling. *Fuel* **2019**, *245*, 594−604.
(54) Malatesta, W. A.; Yang, B. Aviation Turbine Fuel Thermal Conductivity: A Predictive Approach Using Entropy Scaling-Guided Machine Learning with Experimental Validation. *ACS Omega* **2021**, *6* (43), 28579−28586.
(55) Tsederberg, N. V. Thermal Conductivity of Binary Liquid Solutions. *Teploenergetika* **1956**, *3* (9), 42−48.
(56) Lemmon, E. W., Bell, I. H., Huber, M. L., McLinden, M. O. *NIST Standard Reference Database 23: Reference Fluid Thermodynamic and Transport Properties-REFPROP*; National Institute of Standards and Technology (NIST): Gaithersburg, MD 2018.

(57) Baroncini, C.; Latini, G.; Pierpaoli, P. Thermal Conductivity of Organic Liquid Binary Mixtures: Measurements and Prediction Method. *Int. J. Thermophys* **1984**, *5*, 387−401.
(58) Ogiwara, K.; Arai, Y.; Saito, S. Thermal Conductivities of Liquid Hydrocarbons and Their Binary Mixtures. *Ind. Eng. Chem. Fundam.* **1980**, *19* (3), 295−300.
(59) Wada, Y.; Nagasaka, Y.; Nagashima, A. Measurements and Correlation of the Thermal Conductivity of Liquid *n*-Paraffin Hydrocarbons and Their Binary and Ternary Mixtures. *Int. J. Thermophys* **1985**, *6* (3), 251−265.
(60) Boehm, R. C.; Colborn, J. G.; Heyne, J. S. Comparing Alternative Jet Fuel Dependencies Between Combustors of Different Size and Mixing Approaches. *Front. Energy Res.* **2021**, *9*, 701901.
(61) McKinley, G. H.; Renardy, M. Wolfgang von Ohnesorge. *Phys. Fluids* **2011**, *23* (12), 127101.
(62) Hernández, E. A.; Sánchez-Reyna, G.; Ancheyta, J. Evaluation of Mixing Rules to Predict Viscosity of Petrodiesel and Biodiesel Blends. *Fuel* **2021**, *283*, No. 118941.
(63) Arrhenius, S. A. Über die innere Reibung verdünnter wässeriger Lösungen (On the Internal Friction of Dilute Aqueous Solutions). *Z. Phys. Chem.* **1887**, *1U* (1), 285.
(64) Wilding, W. V.; Rowley, R. L.; Oscarson, J. L. DIPPR® Project 801 Evaluated Process Design Data. *Fluid Phase Equilib.* **1998**, *150*−*151* (151), 413−420.
(65) Hugill, J. A.; Van Welsenes, A. J. Surface Tension: A Simple Correlation for Natural Gas + Conensate Systems. *Fluid Phase Equilib.* **1986**, *29* (C), 383−390.
(66) Hammick, D. L.; Andrew, L. W. The Determination of the Parachors of Substances in Solution. *J. Chem. Soc.* **1929**, *0* (0), 754−759.
(67) Schmidt, R. L.; Randall, J. C.; Clever, H. L. The Surface Tension and Density of Binary Hydrocarbon Mixtures: Benzene−*n*-Hexane and Benzene−*n*-Dodecane. *J. Phys. Chem.* **1966**, *70* (12), 3912−3916.
(68) Bezerra, E. S.; Santos, J. M. T.; Paredes, M. L. L. A New Predictive Model for Liquid/Air Surface Tension of Mixtures: Hydrocarbon Mixtures. *Fluid Phase Equilib.* **2010**, *288* (1−2), 55−62.
(69) Boehm, R. C.; Coburn, A. A.; Yang, Z.; Wanstall, C. T.; Heyne, J. S. Blend Prediction Model for the Freeze Point of Jet Fuel Range Hydrocarbons. *Energy Fuels* **2022**, *36* (19), 12046−12053.
(70) Solash, J.; Hazlett, R.; Hall, J.; Nowack, C. Relation between Fuel Properties and Chemical Composition. 1. Jet Fuels from Coal, Oil Shale and Tar Sands. *Fuel* **1978**, *57* (9), 521−528.
(71) Affens, W.; Hall, J.; Holt, S.; Hazlett, R. Effect of Composition on Freezing Points of Model Hydrocarbon Fuels. *Fuel* **1984**, *63* (4), 543−547.
(72) Cookson, D. J.; Lloyd, C. P.; Smith, B. E. Investigation of the Chemical Basis of Kerosene (Jet Fuel) Specification Properties. *Energy Fuels* **1987**, *1* (5), 438−447.
(73) Naef, R. Calculation of the Isobaric Heat Capacities of the Liquid and Solid Phase of Organic Compounds at and around 298.15 K Based on Their "True" Molecular Volume. *Molecules* **2019**, *24* (8), 1626.
(74) Walden, P. Heat of Fusion, Specific Cohesion, and Molecular Complexity at the Melting Point. *Elektrochem* **1908**, *14*, 713.
(75) Hayez, B. Approximate Equation To Calculate Partial Pressures in a Mixture of Real Gases. *J. Chem. Educ.* **2018**, *95* (11), 1982−1988.
(76) Atkins, P. W. *Physical Chemistry*, 3rd.; Freeman and Company: New York, 1986.
(77) Hawkes, S. J. Raoult's Law Is a Deception. *J. Chem. Educ.* **1995**, *72* (3), 204.
(78) Yang, Z.; Bell, D. C.; Cronin, D. J.; Boehm, R.; Heyne, J.; Ramasamy, K. K. Volatility Measurements of Sustainable Aviation Fuels: A Comparative Study of D86 and D2887 Methods. *ACS Sustainable Chem. Eng.* **2024**, *12* (19), 7414−7420.
(79) Le Chatelier, H. Estimation of Firedamp by Flammability Limits. *Ann. Mines* **1891**, *19* (8), 388−395.
(80) Burgess, M. J.; Wheeler, R. V. The Lower Limit of Inflammation of Mixtures of the Paraffin Hydrocarbons with Air. *J. Chem. Soc., Trans.* **1911**, *99*, 2013−2030.
(81) Mashuga, C. V.; Crowl, D. A. Derivation of Le Chatelier's Mixing Rule for Flammable Limits. *Process Saf. Prog.* **2000**, *19* (2), 112−117.
(82) Chen, C.-C.; Liu, S.-H.; Kang, X. Evaluating Lower Flammability Limit of Flammable Mixtures Using Threshold Temperature Approach. *Chem. Eng. Sci.* **2018**, *185*, 84−91.
(83) Coward, H. F.; Jones, G. W. *Limits of Flammability of Gases and Vapors*, 503rd ed.; U.S. Government Printing Office: Washington, D.C., 1952.
(84) Kondo, S.; Takizawa, K.; Takahashi, A.; Tokuhashi, K.; Sekiya, A. A Study on Flammability Limits of Fuel Mixtures. *J. Hazard. Mater.* **2008**, *155* (3), 440−448.
(85) Liekhus, K. J.; Zlochower, I. A.; Cashdollar, K. L.; Djordjevic, S. M.; Loehr, C. A. Flammability of Gas Mixtures Containing Volatile Organic Compounds and Hydrogen. *J. Loss Prev. Process Ind.* **2000**, *13* (3−5), 377−384.
(86) Zabeta, M. G. *Flammability Characteristics of Combustible Gases and Vapors*; Bureau of Mines: Pittsburgh, PA, 1964; DOI: 10.2172/7328370.
(87) National Fire Protection Agency (NFPA). *Fire Protection Guide to Hazardous Materials*; Spencer, A. B., Colonna, G. R., Eds.; NFPA: Quincy, MA, 2002.
(88) Rowley, J. R. Flammability Limits, Flash Points, and Their Consanguinity: Critical Analysis, Experimental Exploration, and Prediction. Ph.D. Thesis, Brigham Young University, Provo, UT, 2010.
(89) Qi, C.; Yan, X.; Wang, Y.; Ning, Y.; Yu, X.; Hou, Y.; Lv, X.; Ding, J.; Shi, E.; Yu, J. Flammability Limits of Combustible Gases at Elevated Temperatures and Pressures: Recent Advances and Future Perspectives. *Energy Fuels* **2022**, *36* (21), 12896−12916.
(90) Phoon, L. Y.; Mustaffa, A. A.; Hashim, H.; Mat, R. A Review of Flash Point Prediction Models for Flammable Liquid Mixtures. *Ind. Eng. Chem. Res.* **2014**, *53* (32), 12553−12565.
(91) Santos, S. M.; Nascimento, D. C.; Costa, M. C.; Neto, A. M. B.; Fregolente, L. V. Flash Point Prediction: Reviewing Empirical Models for Hydrocarbons, Petroleum Fraction, Biodiesel, and Blends. *Fuel* **2020**, *263*, No. 116375.
(92) Wickey, R. O.; Chittenden, D. H. Flash Points of Blends Correlated. *Hydrocarbon Process.* **1963**, *42* (6), 157−158.
(93) Corson, D. R. *Introduction to Electromagnetic Fields and Waves*; W. H. Freeman: San Francisco, CA, 1962; p 116.
(94) Yang, Z.; Bell, D.; Boehm, R.; Fischer Marques, P.; Bose, J.; Kosilkin, I.; Heyne, J. Assessing the Effect of Composition on Dielectric Constant of Sustainable Aviation Fuel. *SSRN* **2024**, 4700499.
(95) Sen, A. D.; Anicich, V. G.; Arakelian, T. Dielectric Constant of Liquid Alkanes and Hydrocarbon Mixtures. *J. Phys. D: Appl. Phys.* **1992**, *25* (3), 516−521.
(96) Teixeira-Dias, J. J. C.; Murrell, J. N. The Calculation of Electric Polarizabilities of Hydrocarbons with Particular Attention to the Bond-Additive Property. *Mol. Phys.* **1970**, *19* (3), 329−335.
(97) Calcote, H. F.; Manos, D. M. Effect of Molecular Structure on Incipient Soot Formation. *Combust. Flame* **1983**, *49* (1−3), 289−304.
(98) Gill, R. J.; Olson, D. B. Estimation of Soot Thresholds for Fuel Mixtures. *Combust. Sci. Technol.* **1984**, *40* (5−6), 307−315.
(99) Yan, S.; Eddings, E. G.; Palotas, A. B.; Pugmire, R. J.; Sarofim, A. F. Prediction of Sooting Tendency for Hydrocarbon Liquids in Diffusion Flames. *Energy Fuels* **2005**, *19* (6), 2408−2415.
(100) Mensch, A.; Santoro, R. J.; Litzinger, T. A.; Lee, S.-Y. Sooting Characteristics of Surrogates for Jet Fuels. *Combust. Flame* **2010**, *157*, 1097−1105.
(101) Yang, Y.; Boehman, A. L.; Santoro, R. J. A Study of Jet Fuel Sooting Tendency Using the Threshold Sooting Index (TSI) Model. *Combust. Flame* **2007**, *149* (1−2), 191−205.
(102) Boehm, R. C.; Yang, Z.; Heyne, J. S. Threshold Sooting Index of Sustainable Aviation Fuel Candidates from Composition Input

Alone: Progress toward Uncertainty Quantification. *Energy Fuels* **2022**, *36*, 1916.
(103) Lemaire, R.; Le Corre, G.; Nakouri, M. Predicting the Propensity to Soot of Hydrocarbons and Oxygenated Molecules by Means of Structural Group Contribution Factors Derived from the Processing of Unified Sooting Indexes. *Fuel* **2021**, *302*, No. 121104.
(104) McEnally, C. S.; Pfefferle, L. D. Improved Sooting Tendency Measurements for Aromatic Hydrocarbons and Their Implications for Naphthalene Formation Pathways. *Combust. Flame* **2007**, *148* (4), 210−222.
(105) ASTM International. *ASTM D02-1531, Diesel Fuel Ignition Quality Tester (IQTTM)—Development of the IQTTM Model to Calculate the Derived Cetane Number (DCN)*; ASTM International: West Conshohocken, PA, 2002.
(106) Colket, M.; Heyne, J. *Fuel Effects on Operability of Aircraft Gas Turbine Combustors*; American Institute of Aeronautics and Astronautics (AIAA): Reston, VA, 2021; DOI: 10.2514/4.106040.
(107) Min, K.; Valco, D. J.; Oldani, A.; Kim, K.; Temme, J.; Kweon, C. B. M.; Lee, T. Autoignition of Varied Cetane Number Fuels at Low Temperatures. *Proc. Combust. Inst.* **2019**, *37* (4), 5003−5011.
(108) Kim, K.; Lee, W.; Wiersema, P.; Mayhew, E.; Temme, J.; Kweon, C.-B. M.; Lee, T. Effects of the Cetane Number on Chemical Ignition Delay. *Energy* **2023**, *264*, No. 126263.
(109) Wang, Y.; Ding, Y.; Wei, W.; Cao, Y.; Davidson, D. F.; Hanson, R. K. On Estimating Physical and Chemical Properties of Hydrocarbon Fuels Using Mid-Infrared FTIR Spectra and Regularized Linear Models. *Fuel* **2019**, *255*, No. 115715.
(110) Al Ibrahim, E.; Farooq, A. Prediction of the Derived Cetane Number and Carbon/Hydrogen Ratio from Infrared Spectroscopic Data. *Energy Fuels* **2021**, *35* (9), 8141−8152.
(111) Boddapati, V.; Ferris, A. M.; Hanson, R. K. On the Use of Extended-Wavelength FTIR Spectra for the Prediction of Combustion Properties of Jet Fuels and Their Constituent Species. *Proc. Combust. Inst.* **2023**, *39* (1), 1347−1355.
(112) Abdul Jameel, A. G.; Naser, N.; Issayev, G.; Touitou, J.; Ghosh, M. K.; Emwas, A.-H.; Farooq, A.; Dooley, S.; Sarathy, S. M. A Minimalist Functional Group (MFG) Approach for Surrogate Fuel Formulation. *Combust. Flame* **2018**, *192*, 250−271.
(113) Heyne, J. S. Direct and Indirect Determinations of Elementary Rate Constants: H + O_2: Chain Branching; the Dehydration of Tertiary-Butanol; the Retro Diels-Alder Reaction of Cyclohexene; the Dehydration of Isopropanol. Ph.D. Thesis, Princeton University, Princeton, NJ, 2014.
(114) Dooley, S.; Won, S. H.; Chaos, M.; Heyne, J.; Ju, Y.; Dryer, F. L.; Kumar, K.; Sung, C.-J.; Wang, H.; Oehlschlaeger, M. A. A Jet Fuel Surrogate Formulated by Real Fuel Properties. *Combust. Flame* **2010**, *157* (12), 2333.
(115) Won, S. H.; Dooley, S.; Veloo, P. S.; Wang, H.; Oehlschlaeger, M. A.; Dryer, F. L.; Ju, Y. The Combustion Properties of 2,6,10-Trimethyl Dodecane and a Chemical Functional Group Analysis. *Combust. Flame* **2014**, *161* (3), 826−834.
(116) Abdul Jameel, A. G.; Naser, N.; Emwas, A.-H.; Dooley, S.; Sarathy, S. M. Predicting Fuel Ignition Quality Using 1H NMR Spectroscopy and Multiple Linear Regression. *Energy Fuels* **2016**, *30* (11), 9819−9835.
(117) Dalmiya, A.; Sheyyab, M.; Mehta, J. M.; Brezinsky, K.; Lynch, P. T. Derived Cetane Number Prediction of Jet Fuels and Their Functional Group Surrogates Using Liquid Phase Infrared Absorption. *Proc. Combust. Inst.* **2023**, *39* (1), 1495−1504.
(118) Faulhaber, C.; Borland, C.; Boehm, R.; Heyne, J. Measurements of Nitrile Rubber Absorption of Hydrocarbons: Trends for Sustainable Aviation Fuel Compatibility. *Energy Fuels* **2023**, *37* (13), 9207−9219.
(119) Romanczyk, M.; Ramirez Velasco, J. H.; Xu, L.; Vozka, P.; Dissanayake, P.; Wehde, K. E.; Roe, N.; Keating, E.; Kilaz, G.; Trice, R. W.; et al. The Capability of Organic Compounds to Swell Acrylonitrile Butadiene O-Rings and Their Effects on O-Ring Mechanical Properties. *Fuel* **2019**, *238*, 483−492.
(120) Liu, Y.; Wilson, C. W. Investigation into the Impact of *n*-Decane, Decalin, and Isoparaffinic Solvent on Elastomeric Sealing Materials. *Adv. Mech. Eng.* **2012**, *4*, 127430.
(121) Graham, J. L.; Striebich, R. C.; Myers, K. J.; Minus, D. K.; Harrison, W. E. Swelling of Nitrile Rubber by Selected Aromatics Blended in a Synthetic Jet Fuel. *Energy Fuels* **2006**, *20* (2), 759−765.
(122) Anuar, A.; Undavalli, V. K.; Khandelwal, B.; Blakey, S. Effect of Fuels, Aromatics and Preparation Methods on Seal Swell. *Aeronaut. J.* **2021**, *125* (1291), 1542−1565.
(123) Kosir, S.; Heyne, J.; Graham, J. A Machine Learning Framework for Drop-in Volume Swell Characteristics of Sustainable Aviation Fuel. *Fuel* **2020**, *274* (April), No. 117832.
(124) Gormley, R. J.; Link, D. D.; Baltrus, J. P.; Zandhuis, P. H. Interactions of Jet Fuels with Nitrile O-Rings: Petroleum-Derived versus Synthetic Fuels. *Energy Fuels* **2009**, *23* (2), 857−861.
(125) Corporan, E.; Edwards, T.; Shafer, L.; Dewitt, M. J.; Klingshirn, C.; Zabarnick, S.; West, Z.; Striebich, R.; Graham, J.; Klein, J. Chemical, Thermal Stability, Seal Swell, and Emissions Studies of Alternative Jet Fuels. *Energy Fuels* **2011**, *25* (3), 955−966.
(126) Hansen, C. M. *The Three Dimensional Solubility Parameter and Solvent Diffusion Coefficient: Their Importance in Surface Coating Formulation*; Danish Technical Press: København, Denmark, 1967.
(127) Ho Manh, L.; Chen, V. C. P.; Rosenberger, J.; Wang, S.; Yang, Y.; Schug, K. A. Prediction of Vacuum Ultraviolet/Ultraviolet Gas-Phase Absorption Spectra Using Molecular Feature Representations and Machine Learning. *J. Chem. Inf Model* **2024**, *64* (14), 5547−5556.
(128) Sheyyab, M.; Lynch, P. T.; Mayhew, E. K.; Brezinsky, K. Optimized Synthetic Data and Semi-Supervised Learning for Derived Cetane Number Prediction. *Combust. Flame* **2024**, *259*, No. 113184.

https://doi.org/10.1021/acs.energyfuels.4c02457
Energy Fuels 2024, 38, 17128−17145